Theory, verification and validation of finite-β gyrokinetics

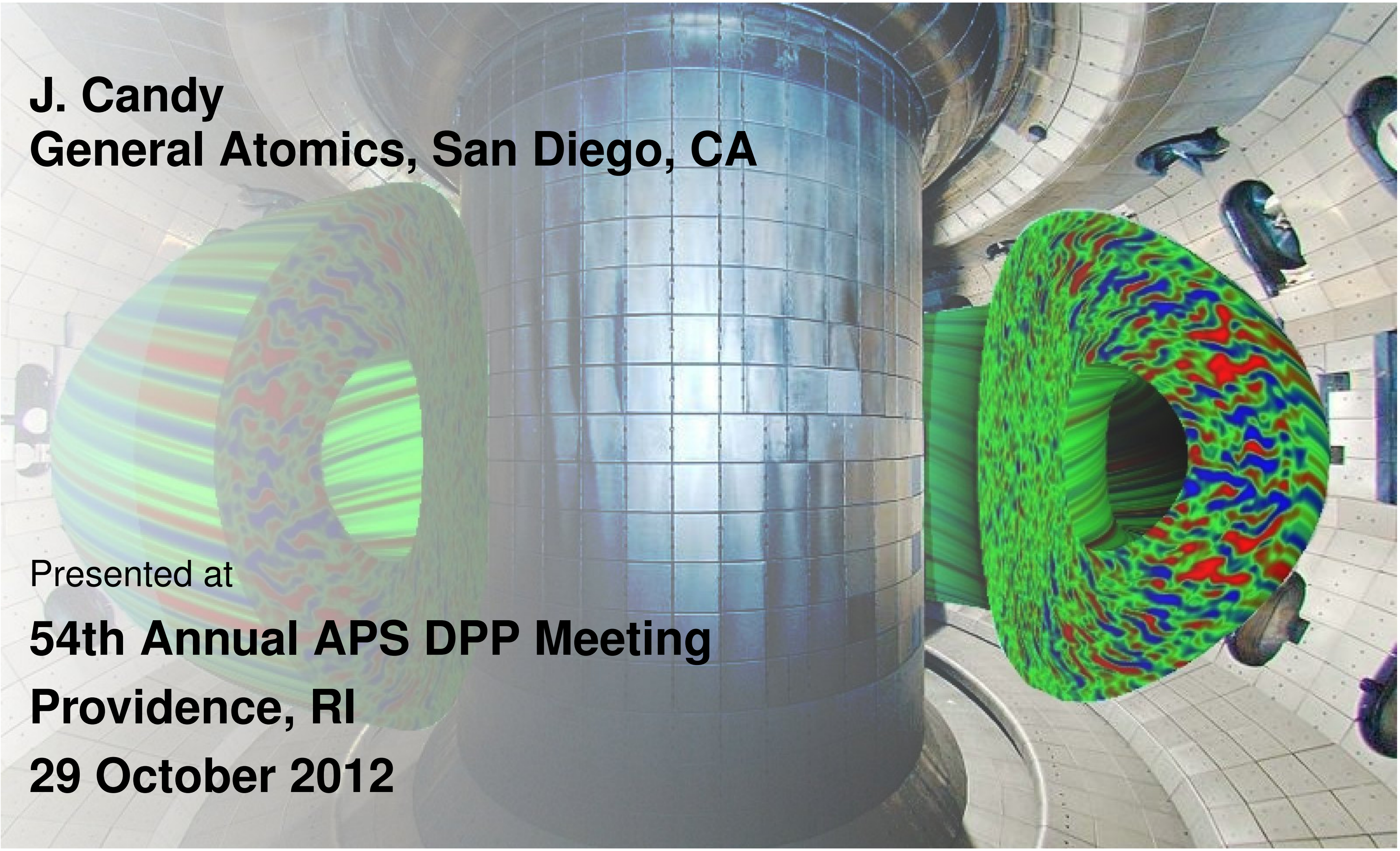

J. Candy
General Atomics, San Diego, CA

Presented at

54th Annual APS DPP Meeting

Providence, RI

29 October 2012

Structure of this Presentation

Role of electromagnetic effects in given contexts

1. Overview of theory and defintions
   - Gyrokinetic equations, transport coefficients, general theory
2. Description of common toroidal eigenmodes
   - Parameteric dependence and eigenmode structure
3. Verification and validation
   - Examples from DIII-D and NSTX
4. Perplexing features of electromagnetic simulation
   - Transport runaway and magnetic stochasticity

Electromagnetic Gyrokinetic Equations

Field dependence through quantity Ψ_a

$$\frac{\partial h_a}{\partial t} + \frac{v_\parallel}{\mathcal{J}_\psi B} \frac{\partial H_a}{\partial \theta} + \mathbf{v}_d \cdot \nabla H_a + \omega_0 \frac{\partial h_a}{\partial \alpha} + c \left[h_a, \Psi_a \right]_{\psi,\alpha}$$

$$+ c \left(\frac{\partial f_{a0}}{\partial \psi} + \frac{m_a v_\parallel}{T_a} \frac{I}{B} \frac{\partial \omega_0}{\partial \psi} f_{a0} \right) \frac{\partial \Psi_a}{\partial \alpha} = C_a^{GL} \left[H_a \right] \ .$$

$$H_a(\mathbf{R}) = \frac{e_a f_{a0}}{T_a} \Psi_a(\mathbf{R}) + h_a(\mathbf{R})$$

$\mathbf{R} \rightarrow$ guiding-center position

$H_a \rightarrow$ nonadiabatic distribution of species a

$f_{a0} \rightarrow$ Maxwellian equilibrium (in frame of rotation) of species a

Gyroaverages of Fields

Compressional potential $\delta B_\parallel$ requires different average

$$\Psi_a(\mathbf{R}) \doteq \left\langle \delta\phi(\mathbf{R}+\boldsymbol{\rho}) - \frac{1}{c}(\mathbf{V}_0+\mathbf{v})\cdot\delta\mathbf{A}(\mathbf{R}+\boldsymbol{\rho}) \right\rangle_{\mathbf{R}} ,$$

$$= \mathcal{G}_{0a}\left[\delta\phi(\mathbf{R}) - \frac{v_\parallel}{c}\delta A_\parallel(\mathbf{R})\right] + \frac{v_\perp^2}{\Omega_{ca}c}\mathcal{G}_{1a}\,\delta B_\parallel(\mathbf{R}) .$$

$\boldsymbol{\rho} = \mathbf{b}\times\mathbf{v}'/\Omega_{ca} \rightarrow$ gyroradius vector

$\Omega_{ca} = e_a B/(m_a c) \rightarrow$ cyclotron frequency

$\delta\phi \rightarrow$ **electrostatic** potential

$\delta A_\parallel \rightarrow$ **transverse electromagnetic** potential

$\delta B_\parallel \rightarrow$ **compressional electromagnetic** potential

Gyroaverages of Fields

Pseudospectral operators valid for all wavelengths

$$\Psi_a(\mathbf{R}) = \mathcal{G}_{0a} \left[\delta\phi(\mathbf{R}) - \frac{v_\parallel}{c} \delta A_\parallel(\mathbf{R}) \right] + \frac{v_\perp^2}{\Omega_{ca} c} \mathcal{G}_{1a}\, \delta B_\parallel(\mathbf{R}) \ .$$

$$z(\mathbf{R}) \doteq \sum_{\mathbf{k}_\perp} e^{iS(\mathbf{R})}\, \tilde{z}(\mathbf{k}_\perp) \ ,$$

$\mathcal{G}_{0a}$ and $\mathcal{G}_{1a}$ are **pseudospectral** operators in real space, with Bessel function representations in wavenumber space:

$$\nabla_\perp^2 \rightarrow -k_\perp^2 \ ,$$

$$\mathcal{G}_{0a} \rightarrow J_0(k_\perp \rho_a) \ ,$$

$$\mathcal{G}_{1a} \rightarrow \frac{1}{2} \left[J_0(k_\perp \rho_a) + J_2(k_\perp \rho_a) \right] \ .$$

Electromagnetic Maxwell Equations

$\mathtt{N\_FIELD} = 1, 2, 3$

Poisson equation

$$-\nabla_\perp^2 \delta\phi(\mathbf{x}) = 4\pi \sum_a e z_a \, \delta n_a = 4\pi \sum_a e_a \int d^3v \, \hat{f}_{a1}(\mathbf{x}) \ .$$

Parallel Ampère's Law

$$-\nabla_\perp^2 \delta A_\parallel(\mathbf{x}) = \frac{4\pi}{c} \sum_a \delta j_{\parallel,a} = \frac{4\pi}{c} \sum_a e_a \int d^3v \, v_\parallel \, \hat{f}_{a1}(\mathbf{x}) \ .$$

Perpendicular Ampère's Law

$$\nabla_\perp \delta B_\parallel(\mathbf{x}) \times \mathbf{b} = \frac{4\pi}{c} \sum_a \delta \mathbf{j}_{\perp,a} = \frac{4\pi}{c} \sum_a e_a \int d^3v \, \mathbf{v}_\perp \hat{f}_{a1}(\mathbf{x})$$

Overview and General Considerations

Connecting particle distribution to gyrocenter distribution

Right-hand sides can be written in terms of H_a

$$\int d^3v\, \hat{f}_{a1}(\mathbf{x}) = -\frac{n_a e_a}{T_a}\,\delta\phi(\mathbf{x}) + \int d^3v\, H_a(\mathbf{x}-\boldsymbol{\rho}) \ ,$$

$$\int d^3v\, v_\parallel\, \hat{f}_{a1}(\mathbf{x}) = \int d^3v\, v_\parallel\, H_a(\mathbf{x}-\boldsymbol{\rho})$$

$$\int d^3v\, \mathbf{v}_\perp\, \hat{f}_{a1}(\mathbf{x}) = \int d^3v\, \mathbf{v}_\perp\, H_a(\mathbf{x}-\boldsymbol{\rho})$$

$\hat{f}_{a1}(\mathbf{x}) \rightarrow$ fluctuating part of perturbed **6-D distribution**

$\mathbf{x} = \mathbf{R} + \boldsymbol{\rho} \rightarrow$ particle position

Flux surfaces labeled by effective minor radius, r.

Generalises the Waltz-Miller midplane minor radius

r is the **half-width** of the flux-surface at the elevation of the centroid.

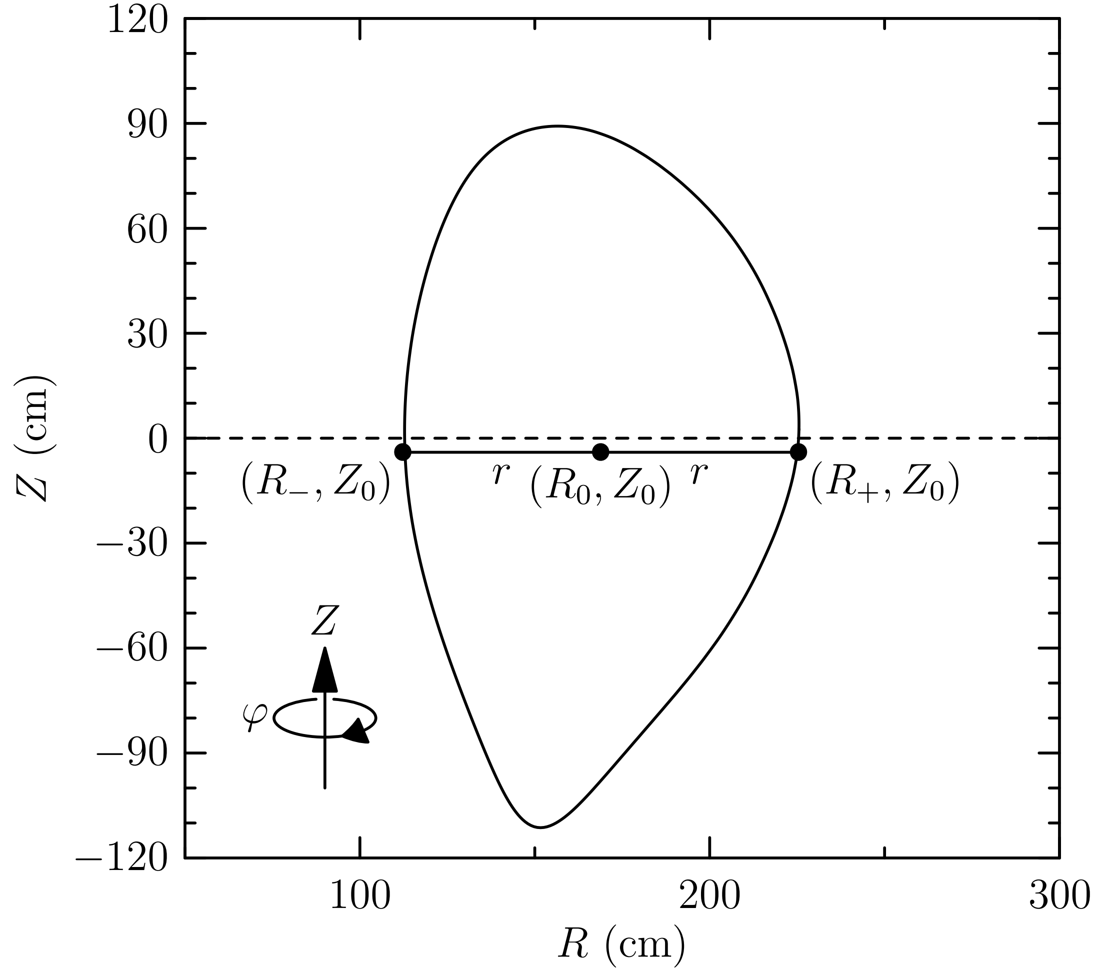

GENERAL ATOMICS

The effective field $B_{\rm unit}$ and other flux functions

Meaning is perpetual source of confusion for users

- $B_{\rm unit}$ is the **effective magnetic field**.

$$B_{\rm unit}(r) \doteq \frac{1}{r}\frac{d\chi_t}{dr} = \frac{q}{r}\frac{d\psi}{dr} \; .$$

- Arguably the most **elegant** choice for local simulations

- Effective gyroradius

$$\rho_{s,\rm unit} = \frac{c_s}{eB_{\rm unit}/(m_i c)}$$

- Effective electron beta

$$\beta_{e,\rm unit} = \frac{8\pi n_e T_e}{B_{\rm unit}^2}$$

Transport Coefficients

Suitable ensemble averages, $\langle\!\langle \cdot \rangle\!\rangle$, must be taken

$$\Gamma_a = \frac{c}{\psi'} \left\langle\!\!\left\langle \int d^3v \, H_a^*(\mathbf{R}) \, \frac{\partial \Psi_a}{\partial \alpha} \right\rangle\!\!\right\rangle ,$$

$$Q_a = \frac{c}{\psi'} \left\langle\!\!\left\langle \int d^3v \, H_a^*(\mathbf{R}) \, \frac{1}{2} m_a v^2 \, \frac{\partial \Psi_a}{\partial \alpha} \right\rangle\!\!\right\rangle ,$$

$$\Pi_a = \frac{c}{\psi'} \left\langle\!\!\left\langle \int d^3v \, H_a^*(\mathbf{R}) m_a R \left[\left(V_0 + v_\parallel \frac{B_t}{B} \right) \frac{\partial \Psi_a}{\partial \alpha} + v_\perp \frac{B_p}{B} \frac{\partial \mathcal{X}_a}{\partial \alpha} \right] \right\rangle\!\!\right\rangle ,$$

$$S_a = \frac{c}{\psi'} \left\langle\!\!\left\langle \int d^3v \, H_a^*(\mathbf{R}) \, e_a \left(\frac{\partial}{\partial t} + \omega_0 \frac{\partial}{\partial \alpha} \right) \Psi_a \right\rangle\!\!\right\rangle .$$

$$\langle\!\langle \, \cdot \, \rangle\!\rangle \doteq \lim_{t_* \to \infty} \frac{1}{2\pi L \, \tau} \int_o^L dr \int_0^{2\pi} d\alpha \int_0^{\tau} dt \; \mathcal{F} \cdot \; ,$$

GENERAL ATOMICS

Transport Coefficients

GyroBohm normalizations

$$\Gamma_a \to \Gamma_{\mathrm{GB}} \doteq n_e c_s (\rho_{s,\mathrm{unit}}/a)^2$$

$$Q_a \to Q_{\mathrm{GB}} \doteq n_e c_s T_e (\rho_{s,\mathrm{unit}}/a)^2$$

$$\Pi_a \to \Pi_{\mathrm{GB}} \doteq n_e a T_e (\rho_{s,\mathrm{unit}}/a)^2$$

$$S_a \to S_{\mathrm{GB}} \doteq n_e (c_s/a) T_e (\rho_{s,\mathrm{unit}}/a)^2$$

Form of Maxwell Equations used in Practice

Poisson equation

$$-\frac{1}{4\pi}\nabla_\perp^2\delta\phi + \sum_a n_a \frac{e_a^2}{T_a}\int d^3v\, F_{Ma}\,(1-\mathcal{G}_{0a}^2)\delta\phi$$

$$-\sum_a n_a \frac{e_a^2}{T_a}\int d^3v\, F_{Ma}\mathcal{G}_{0a}\mathcal{G}_{1a}\frac{v_\perp^2}{\Omega_{ca}c}\,\delta B_\parallel = \sum_a e_a \int d^3v\, \mathcal{G}_{0a} h_a$$

Parallel Ampère's Law

$$-\frac{1}{4\pi}\nabla_\perp^2\delta A_\parallel + \sum_a n_a \frac{e_a^2}{T_a}\int d^3v\, \frac{v_\parallel^2}{c^2} F_{Ma}\mathcal{G}_{0a}^2\delta A_\parallel = \sum_a e_a \int d^3v\, \frac{v_\parallel}{c}\mathcal{G}_{0a} h_a$$

Perpendicular Ampère's Law

$$\frac{1}{4\pi}\delta B_\parallel + \sum_a n_a \frac{e_a^2}{T_a}\int d^3v\, F_{Ma}\left(\frac{v_\perp^2}{\Omega_{ca}c}\mathcal{G}_{1a}\right)^2 \delta B_\parallel$$

$$+\sum_a n_a \frac{e_a^2}{T_a}\int d^3v\, F_{Ma}\frac{v_\perp^2}{\Omega_{ca}c}\mathcal{G}_{1a}\mathcal{G}_{0a}\delta\phi = -\sum_a e_a \int d^3v\, \mathcal{G}_{1a}\frac{v_\perp^2}{\Omega_{ca}c} h_a$$

The Ampère Cancellation Problem

- Let's assume a pure plasma with $T_i = T_e$ and $k_\perp \rho_{s,\mathrm{unit}} \ll 1$:

$$-\frac{2k_\perp^2 \rho_{s,\mathrm{unit}}^2}{\beta_{e,\mathrm{unit}}} \delta \hat{A}_\parallel + \left(1 + \frac{m_i}{m_e}\right) \delta \hat{A}_\parallel = \sum_a e_a \int d^3v \, \hat{v}_{\parallel a} \hat{h}_a$$

- The factor m_i/m_e is **artificial**.
- It is cancelled by a corresponding term in $\hat{h}_a$.
- Attempting to perform field integral analytically will lead to **pain**.
- Must devise a numerical scheme for which artificial pieces **cancel**.

Scaling parameters to control finite-β effects

`AMPERE_SCALE` and `GEO_BETAPRIME_SCALE`

Finite-β effects appear in two different ways/places:

1. **Magnetic fluctuations:** $\beta_{e,\mathrm{unit}} \rightarrow \mathtt{AMPERE\_SCALE} \times \beta_{e,\mathrm{unit}}$

$$-\frac{2\rho_{s,\mathrm{unit}}^2}{\beta_{e,\mathrm{unit}}}\nabla_\perp^2 \delta\hat{A}_\parallel + \sum_a \alpha_a z_a^2 V[\hat{v}_{\parallel a}^2 \mathcal{G}_{0a}^2 \delta\hat{A}_\parallel] = \sum_a z_a V[\hat{v}_{\parallel a}\mathcal{G}_{0a}\hat{h}_a]$$

2. **Geometry/drift motion:** $\nabla p \rightarrow \mathtt{GEO\_BETAPRIME\_SCALE} \times \nabla p$

$$\mathbf{v}_d = \frac{v_\parallel^2 + \mu B}{\Omega_{ca} B}\mathbf{b}\times\nabla B + \frac{2v_\parallel \omega_0}{\Omega_{ca}}\mathbf{b}\times\mathbf{s} + \frac{4\pi v_\parallel^2}{\Omega_{ca}B^2}\mathbf{b}\times\nabla p$$

Working with experimental data:

Workflow enabled with `profiles_gen` command-line tool

```
$ profiles_gen -i iterdb
```

Supported interfaces for **reading profile data** from:

1. ITERDB ASCII
2. ITERDB NetCDF
3. Plasma State NetCDF
4. CORSICA ASCII
5. ASTRA ASCII
6. PEQDSK/ELITE ASCII
7. UFILE (ITPA database)

Working with experimental data:

Options for `profiles_gen` usage: EFIT gfile

- GATO mapper automatically extracts high-resolution flux surfaces
- Fitter simultaneously generates **model (Miller-type)** fit

$$R(r,\theta) = R_0(r) + r\cos(\theta + \arcsin\delta\sin\theta) \ ,$$

$$Z(r,\theta) = Z_0(r) + \kappa r\sin(\theta + \zeta\sin 2\theta) \ ,$$

- And **general (up-down asymmetric)** fit

$$R(r,\theta) = \frac{1}{2}\,a_0^R(r) + \sum_{n=1}^{N}\left[a_n^R(r)\cos(n\theta) + b_n^R(r)\sin(n\theta)\right] \ ,$$

$$Z(r,\theta) = \frac{1}{2}\,a_0^Z(r) + \sum_{n=1}^{N}\left[a_n^Z(r)\cos(n\theta) + b_n^Z(r)\sin(n\theta)\right] \ .$$

Working with experimental data:

General fit only required close to separatrix ($r/a = 0.99$ shown below)

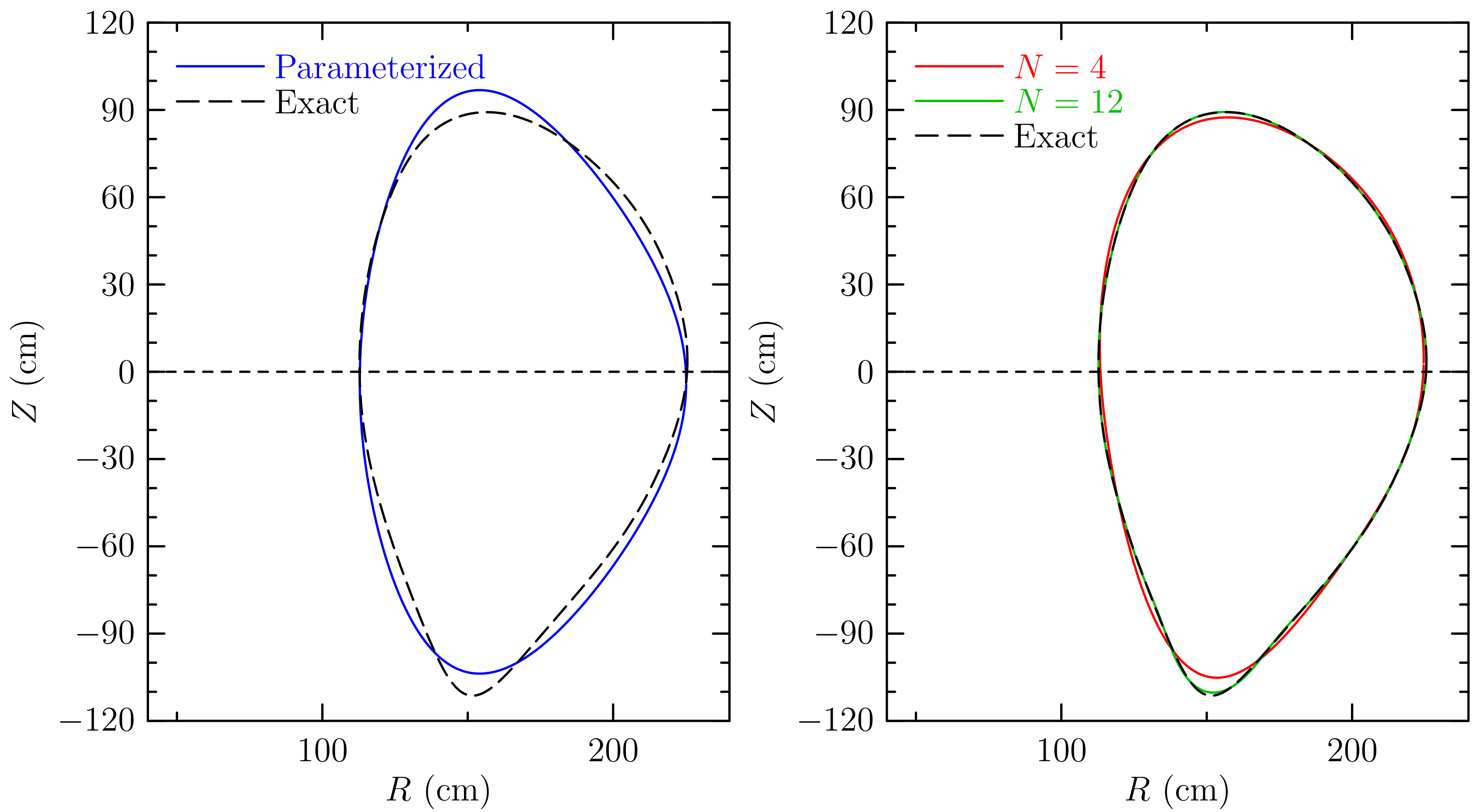

GENERAL ATOMICS

Working with experimental data:

Options for `profiles_gen` usage: NEO calculation of E_r

- Use **NEO** to compute rotation profile

$$\omega_0(r) = \frac{cE_r}{RB_p} = -c\frac{\partial\Phi}{\partial\psi}$$

- Calculation unique given **measured Carbon** $v_{\phi,c}(r)$ profile.
- Logic for handling multiple ions, species lumping, sonic rotation, etc.
- **Diagnostic** calculation of **all** ion velocities: $v_{\phi,a}$, $v_{\theta,a}$.

GA Standard Case (Miller circle) β scan

$\alpha_{\mathrm{MHD}} = 0$

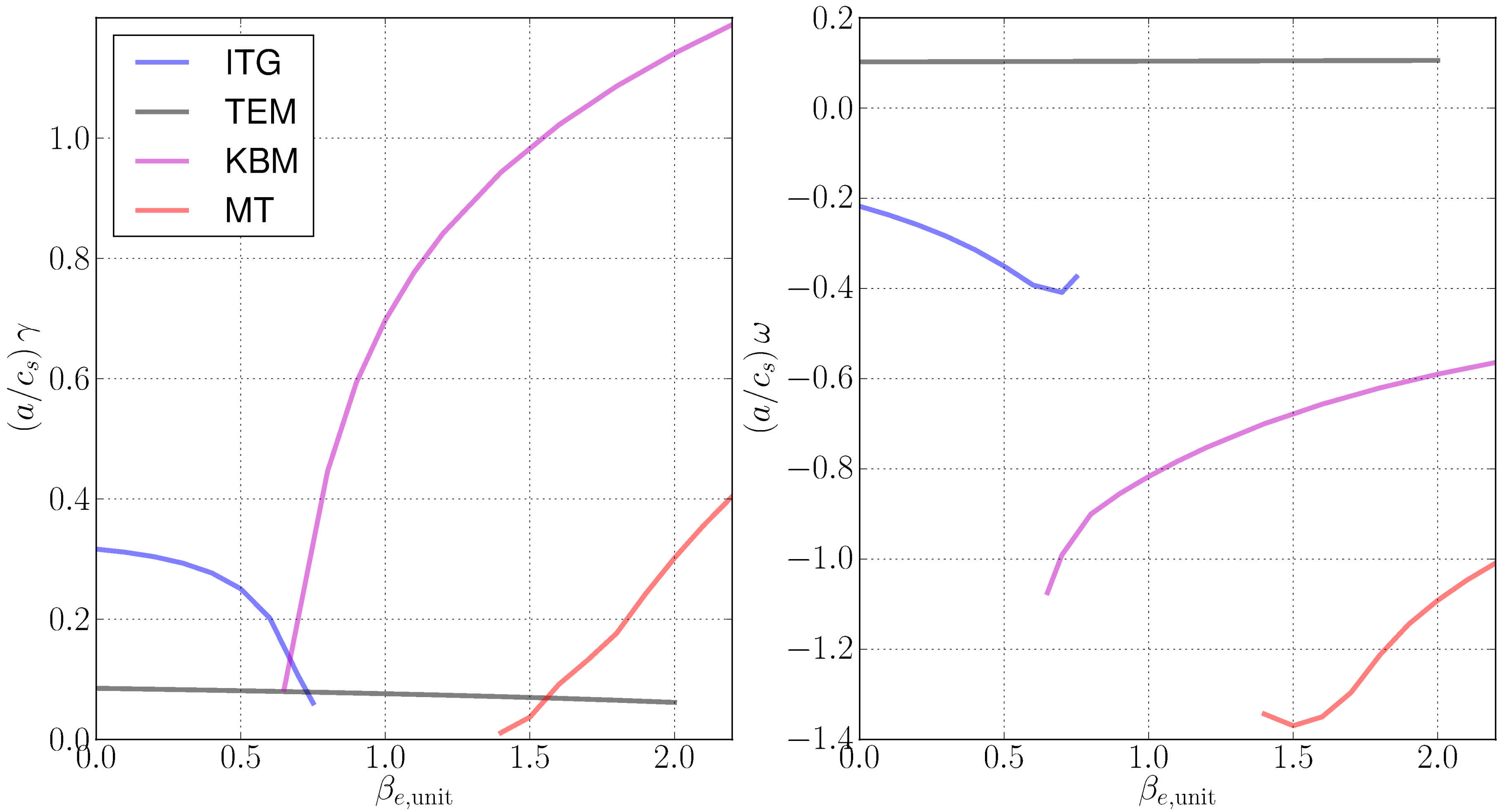

Ion Temperature Gradient (ITG) Mode

$\beta_e = 0.2\%, \alpha_{\mathrm{MHD}} = 0$

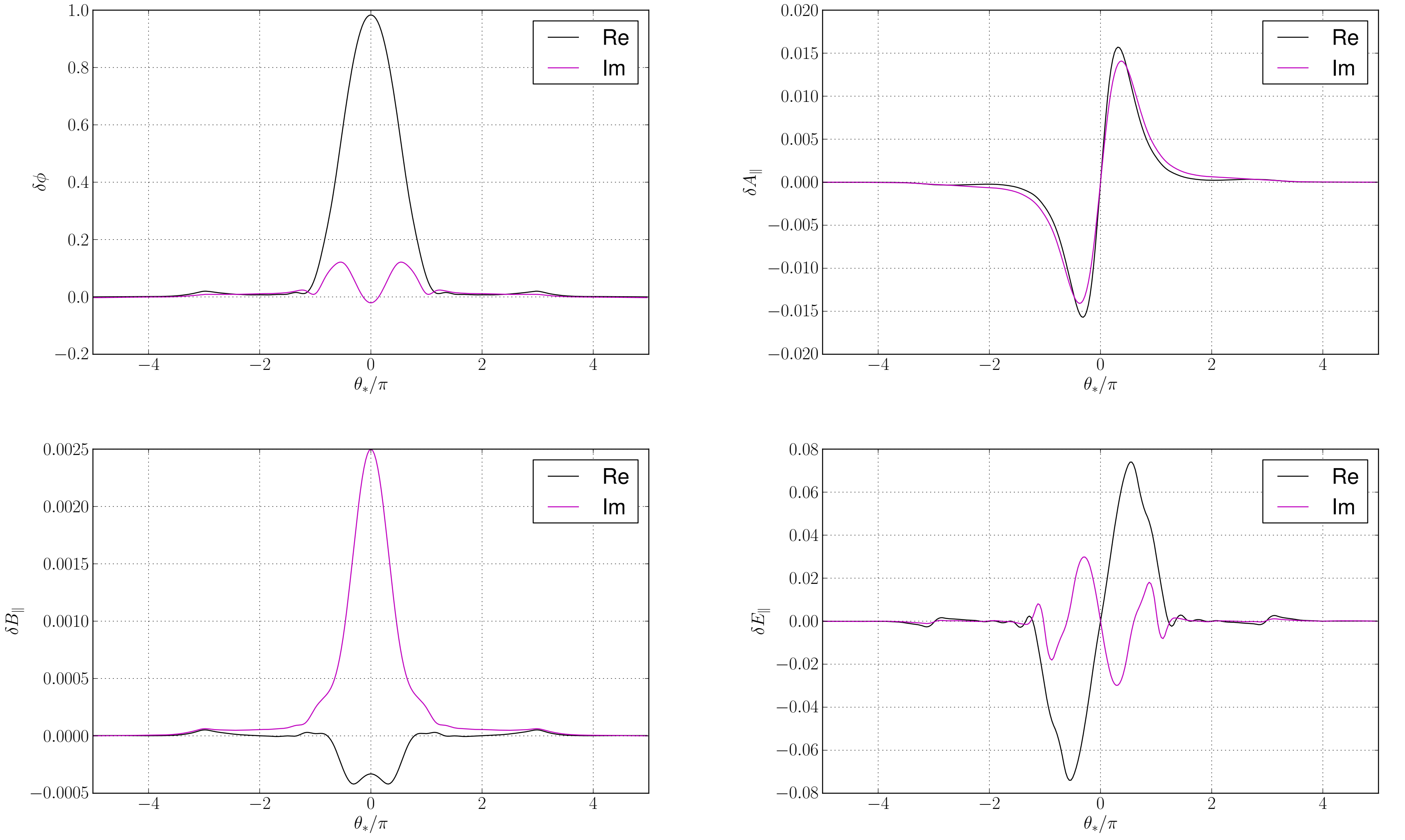

GENERAL ATOMICS

Trapped Electron Mode (TEM)

$\beta_e = 0.2\%, \alpha_{\mathrm{MHD}} = 0$

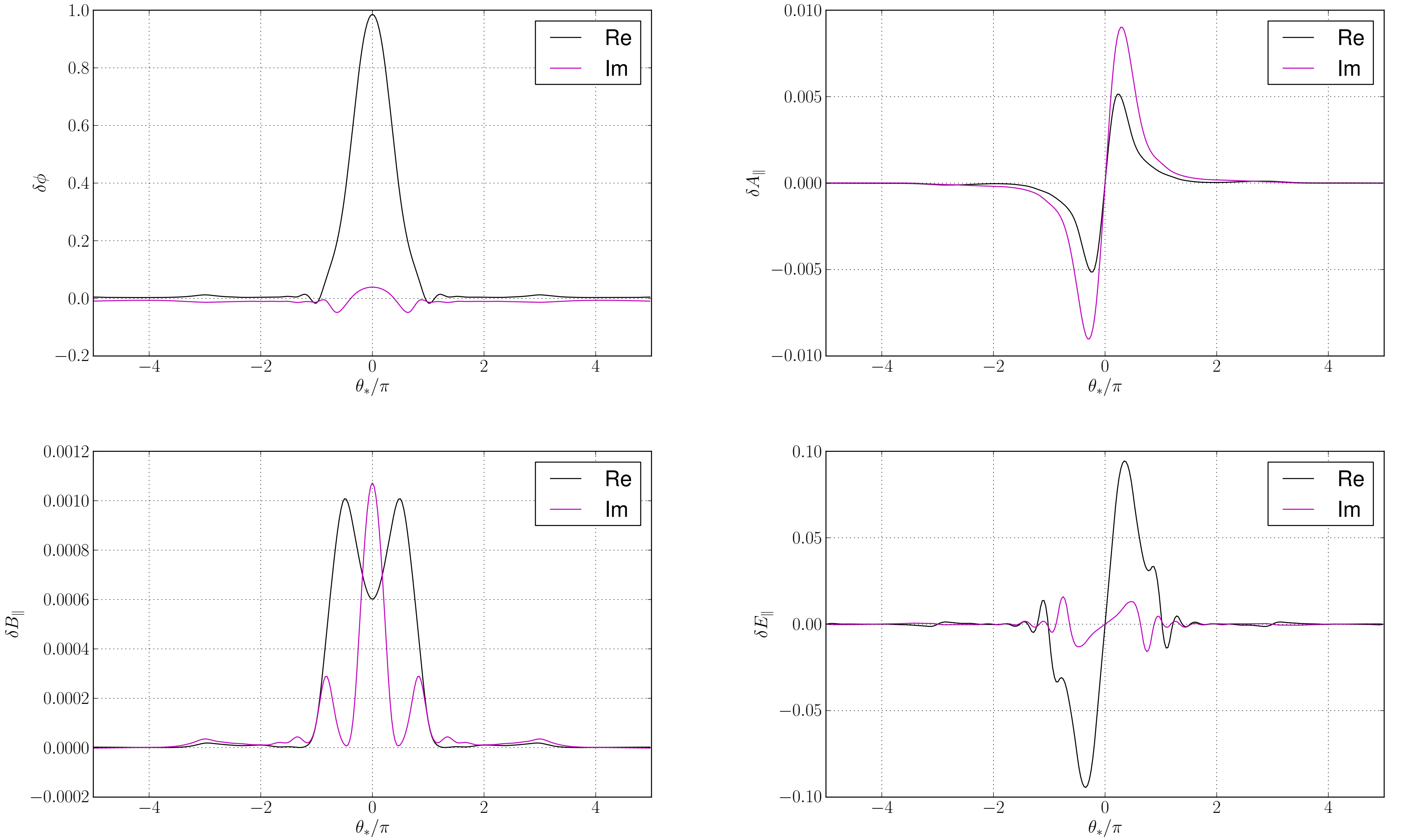

Kinetic Ballooning Mode (KBM)

$\beta_e = 2.2\%, \alpha_{\mathrm{MHD}} = 0$

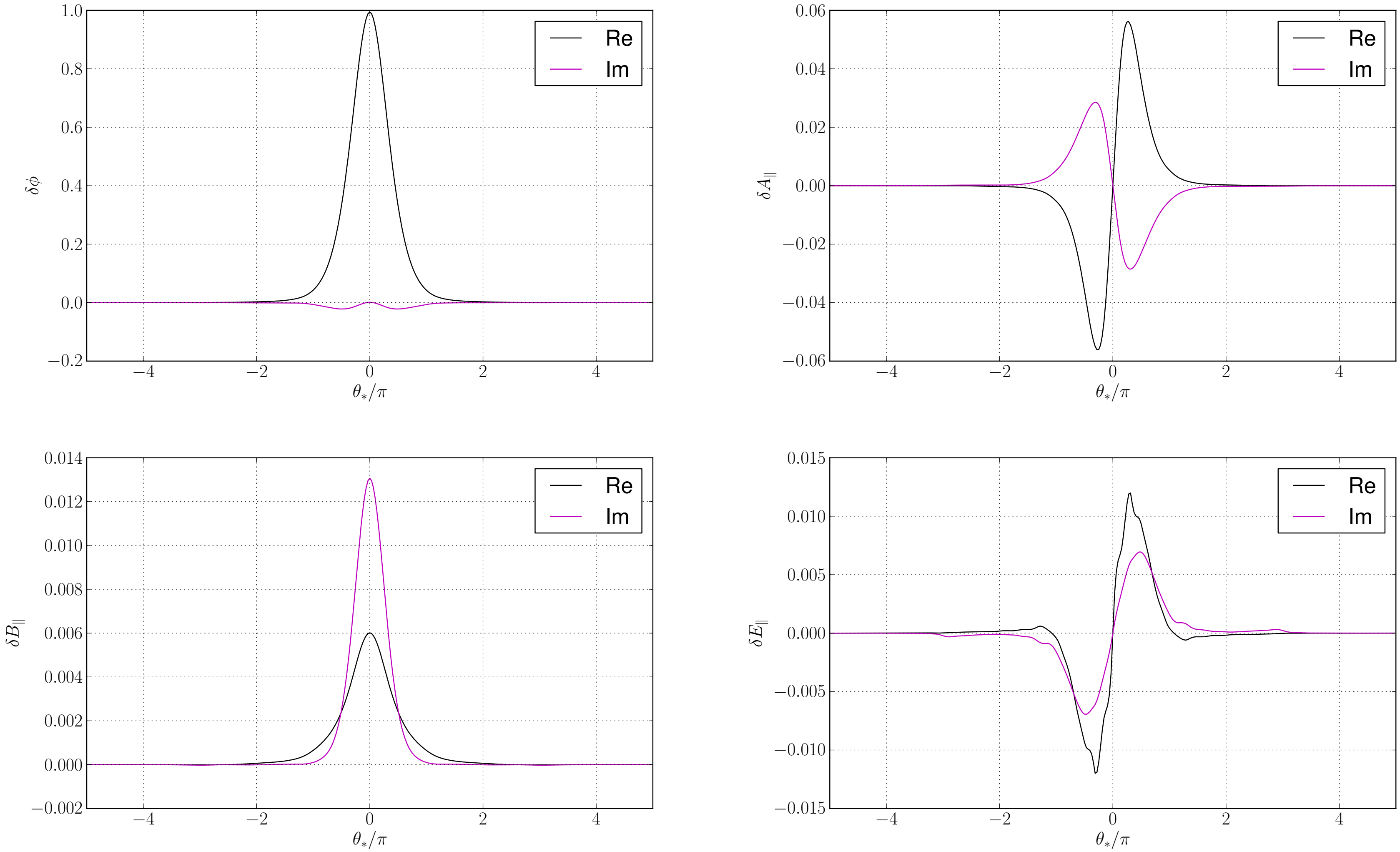

GENERAL ATOMICS

Tearing-parity mode (TPM)

$\beta_e = 2.2\%$, $\alpha_{\mathrm{MHD}} = 0$

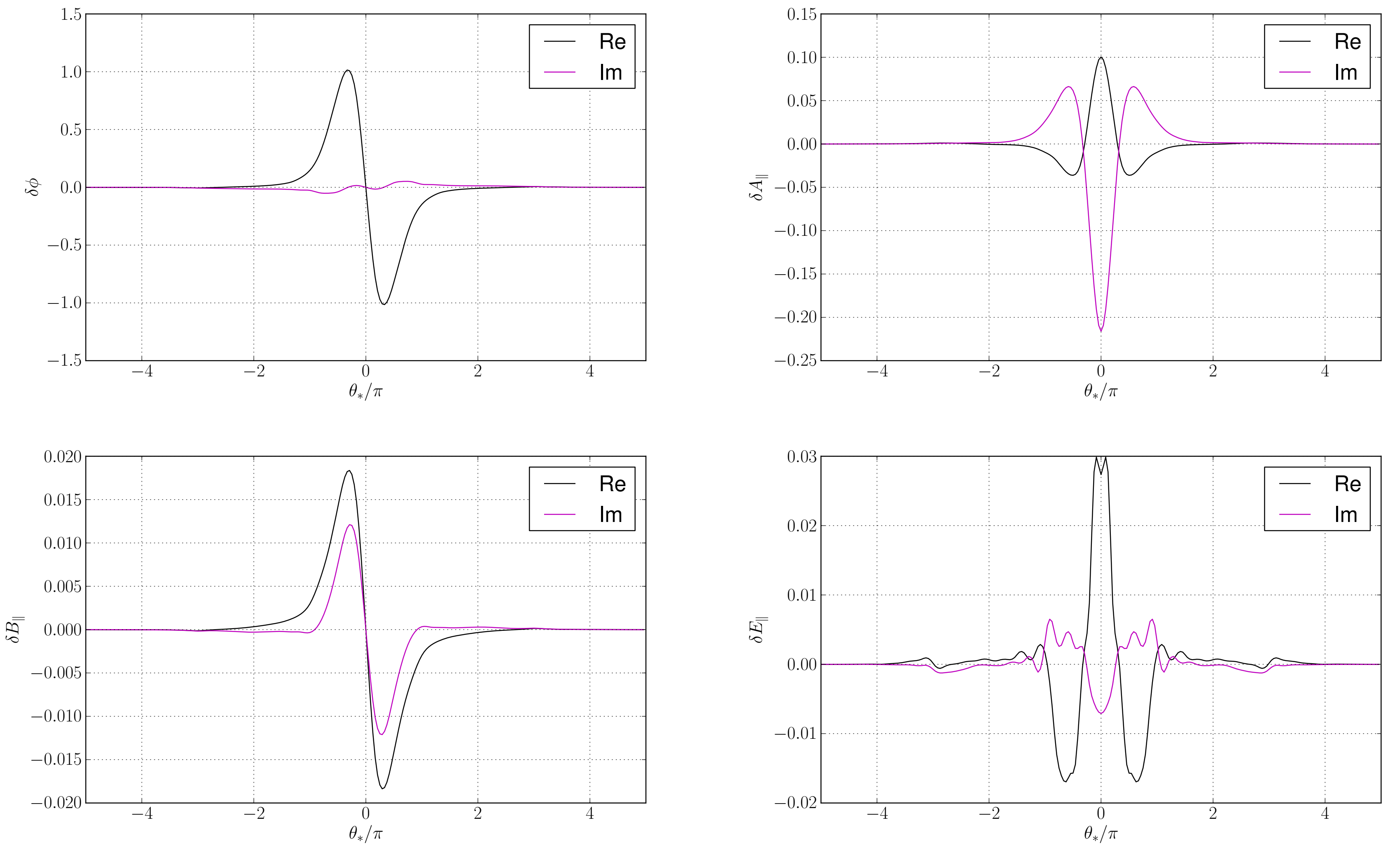

GA Standard Case β scan

Self-consistent α_{MHD}

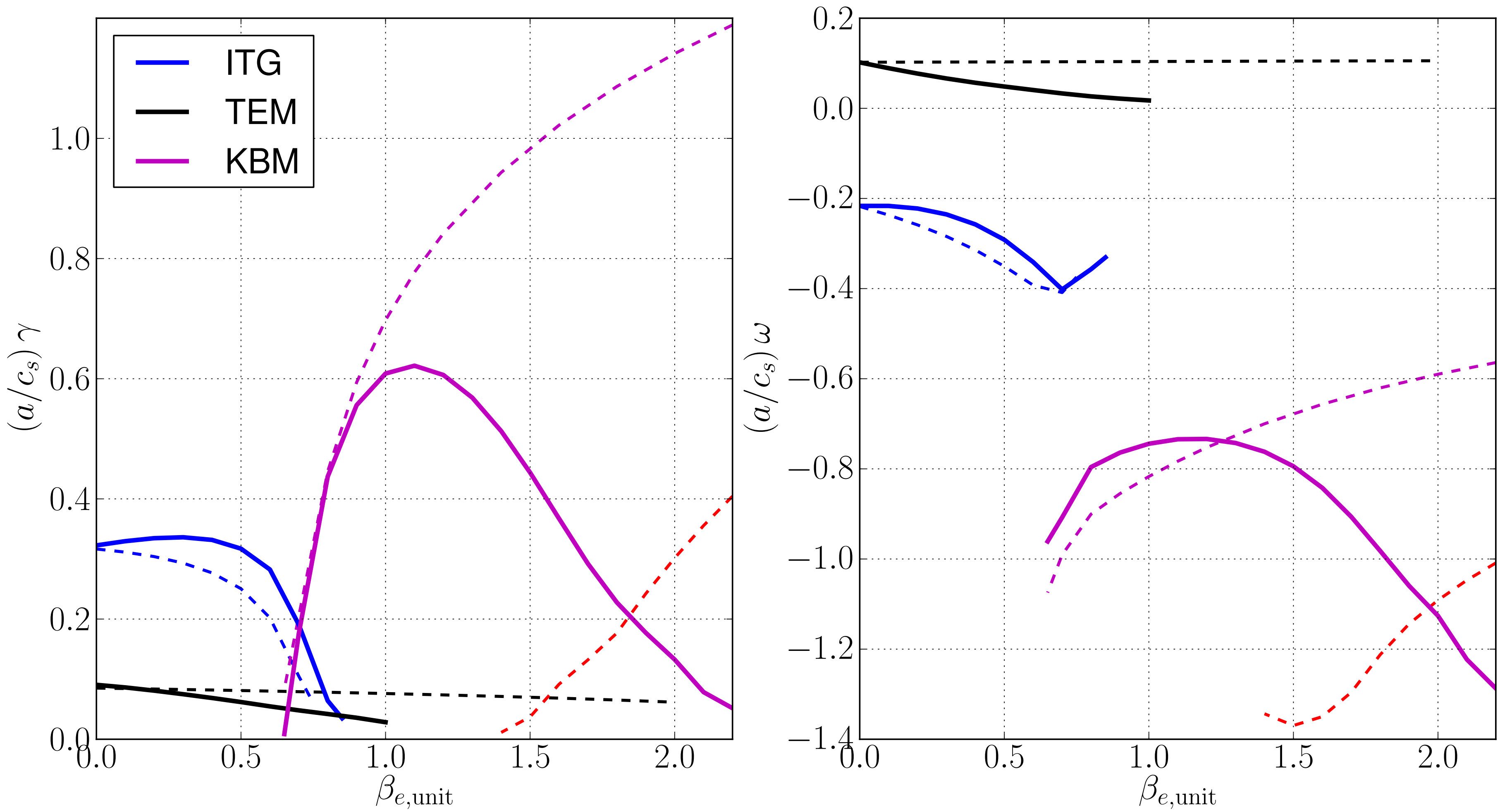

Ion temperature gradient scan

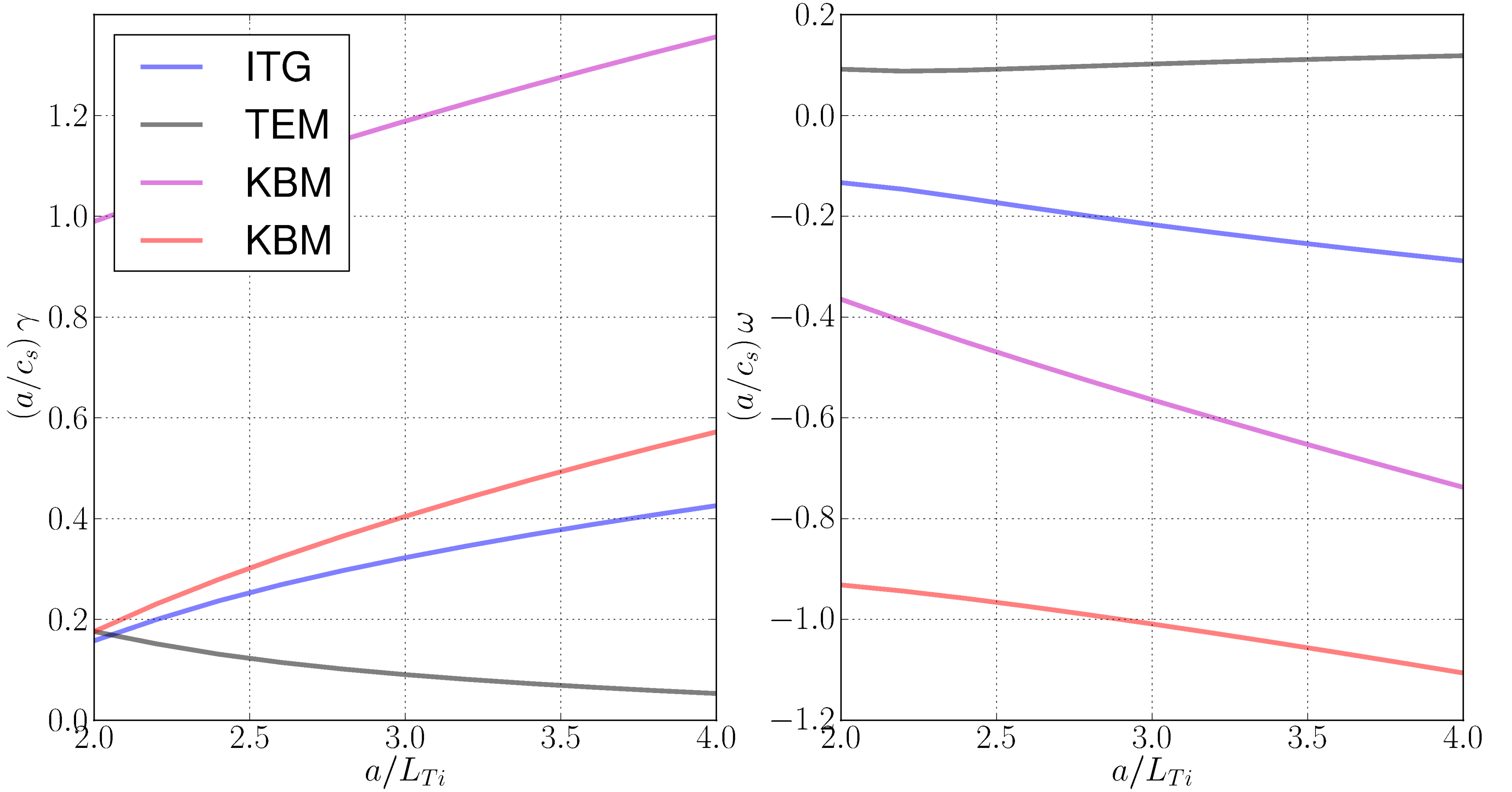

Electron temperature gradient scan

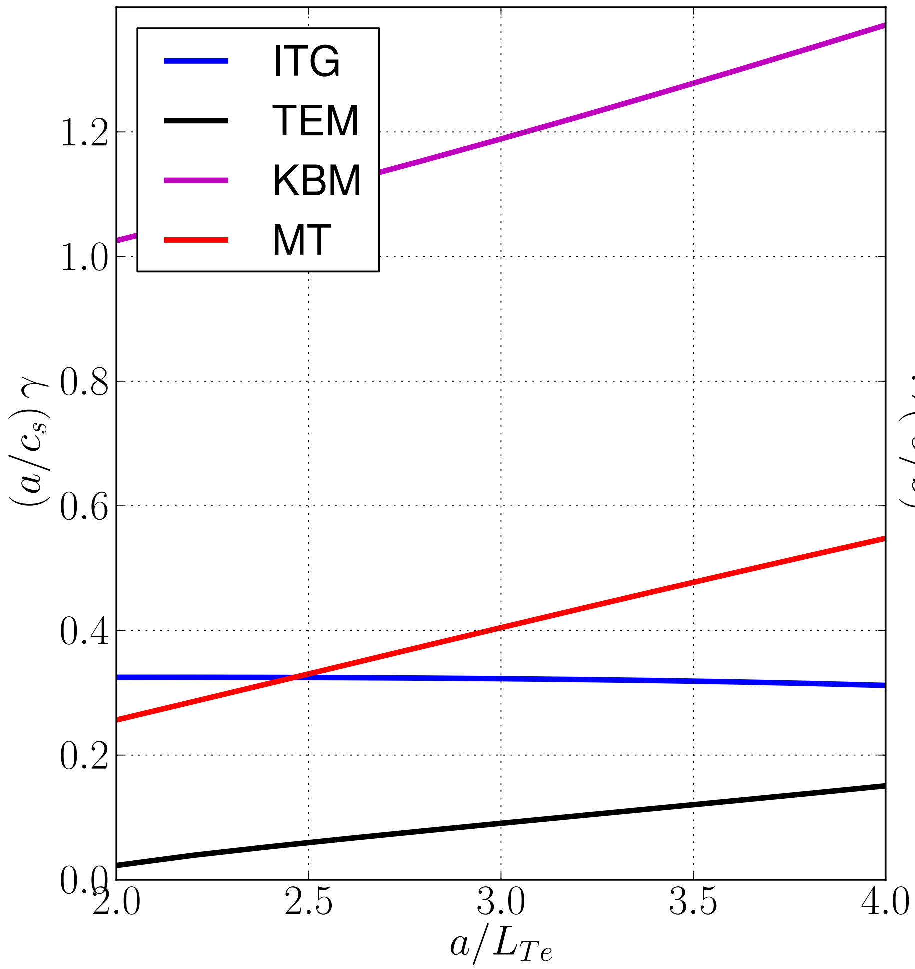

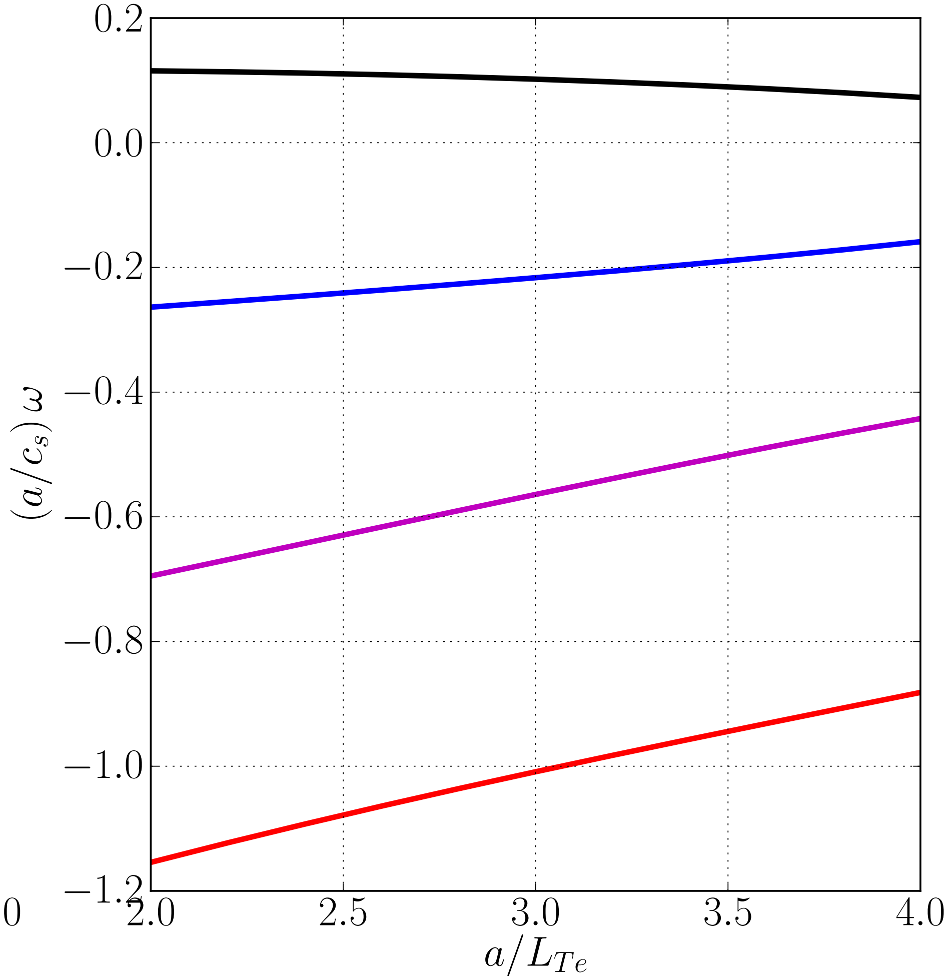

GENERAL ATOMICS

Density gradient scan

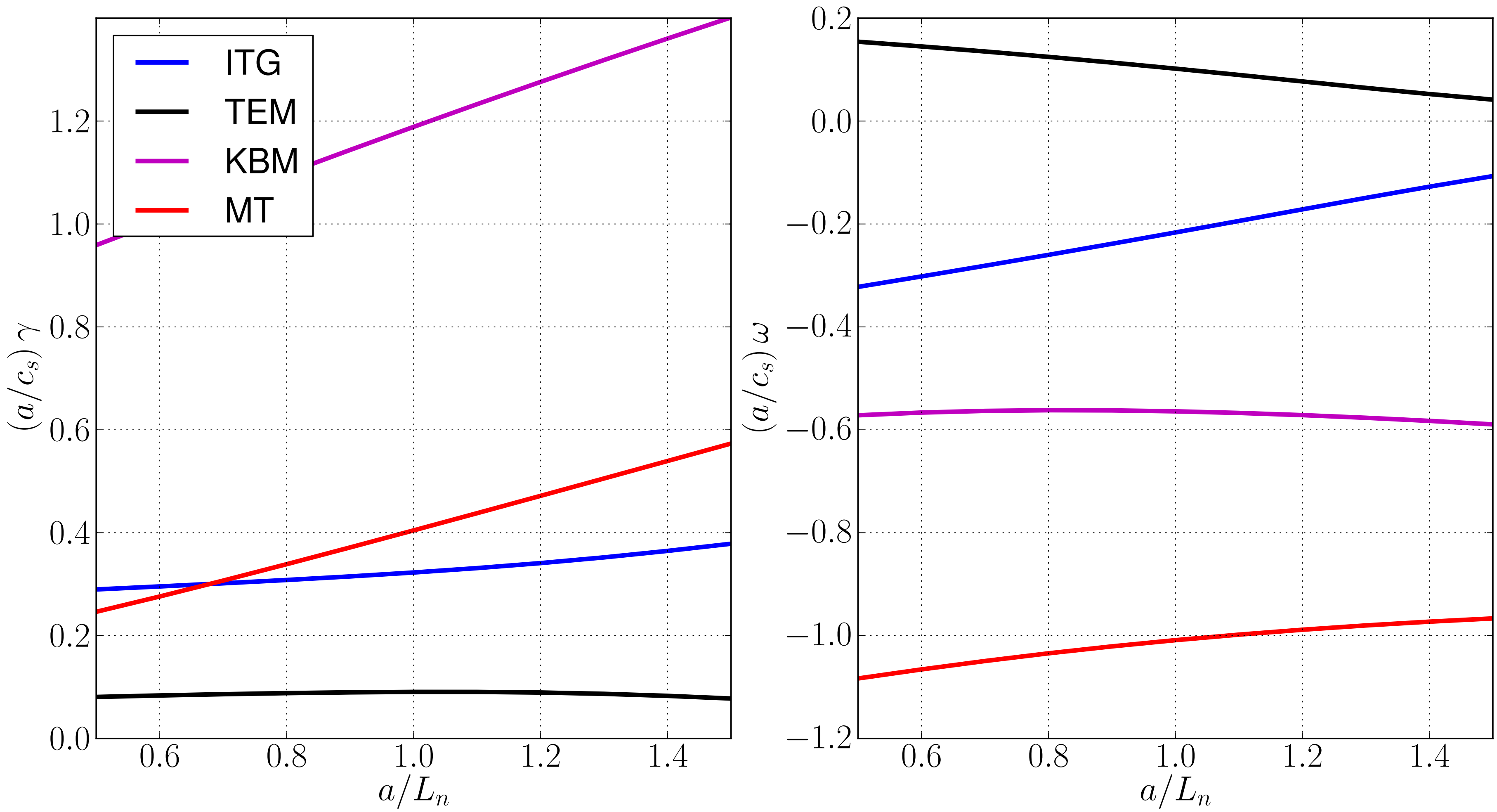

Collision frequency scan

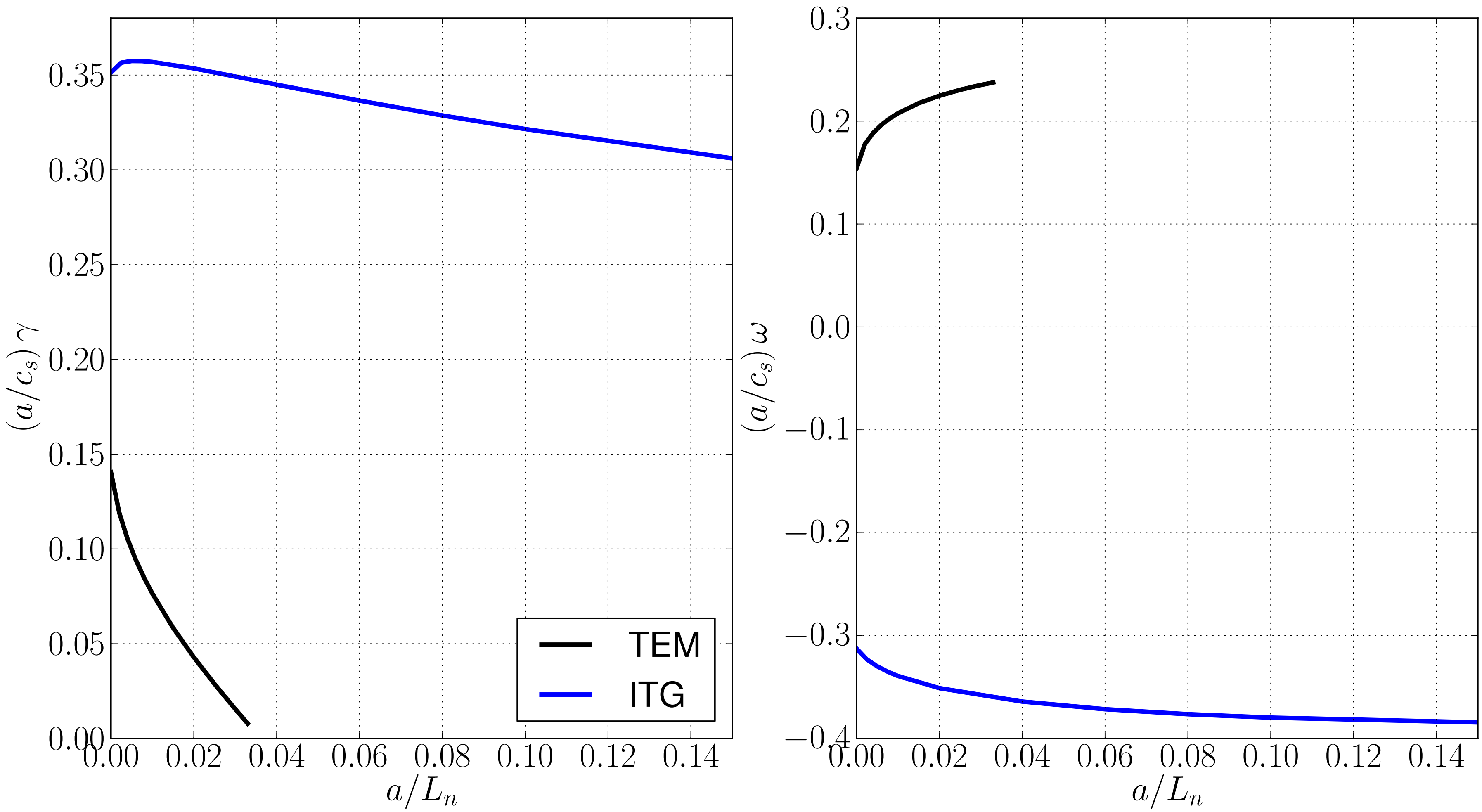

Finite-β version of the Cyclone Case

Belli POP 2010

MHD critical beta occurs at about $\beta_{e,\mathrm{unit}} \simeq 1.2\%$

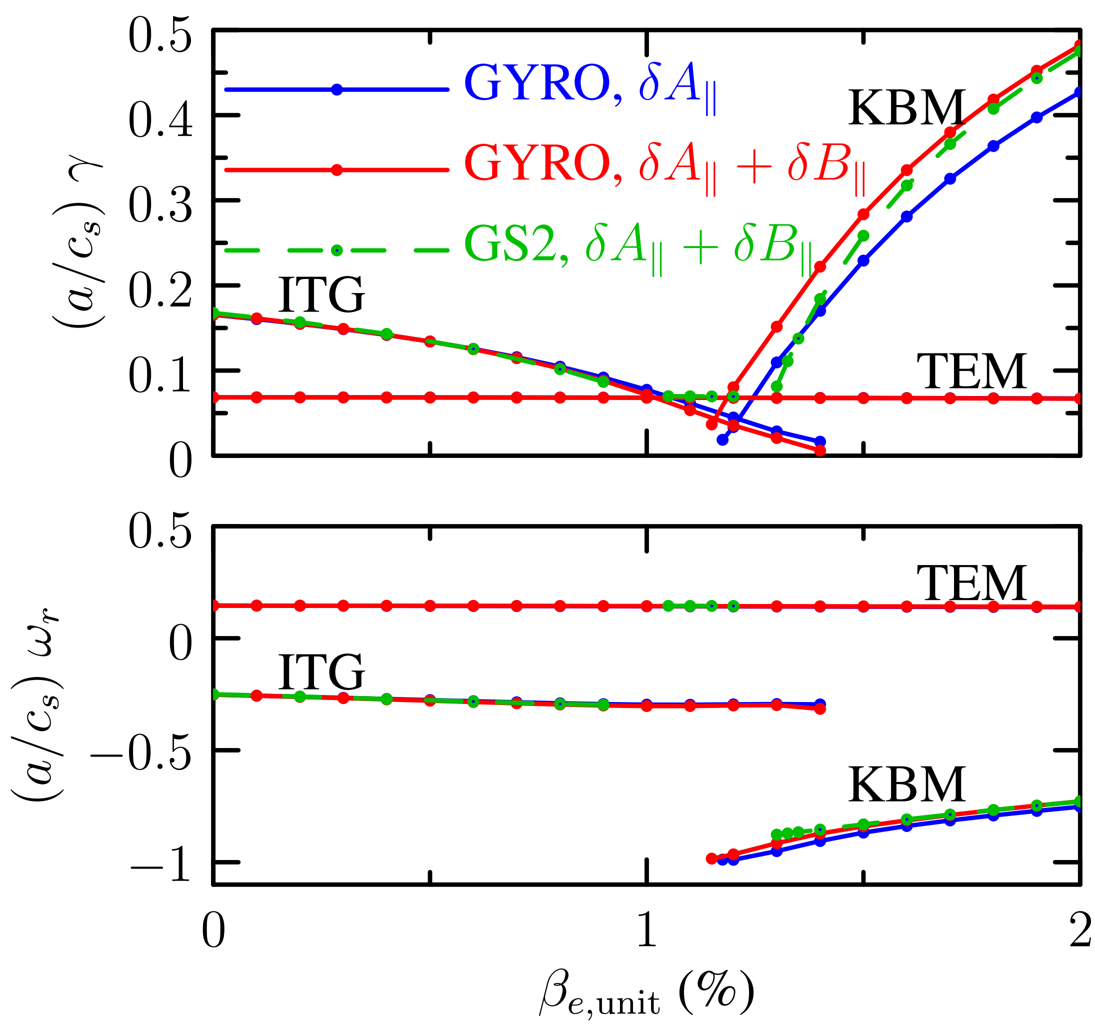

Excellent GYRO-GS2 agreement on Holland validation case

Bravenec PoP 2011: Revisit DIII-D 128913 at $\rho = 0.5$

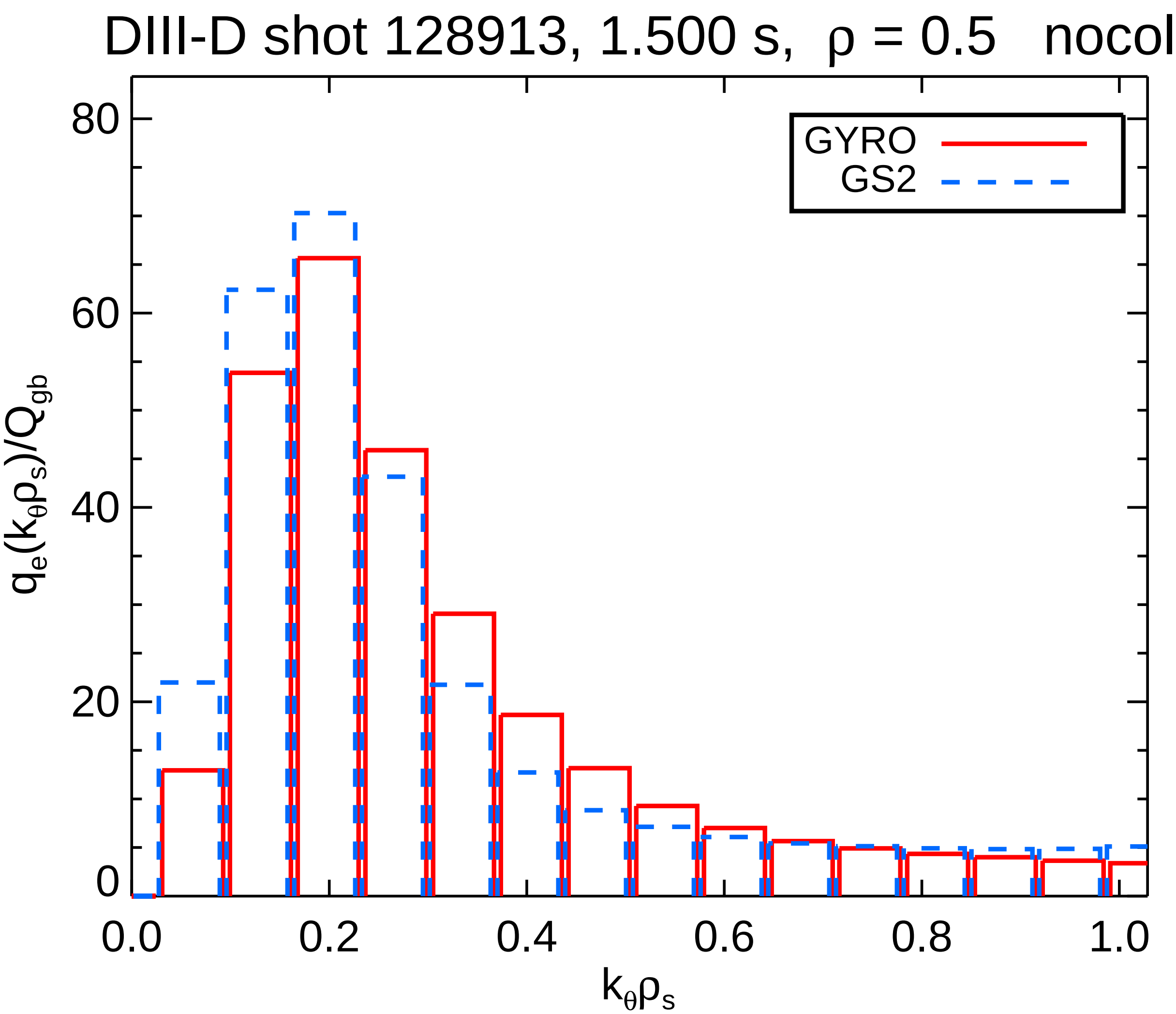

Excellent GYRO-GS2 agreement on Holland validation case

Bravenec PoP 2011: Good agreement in all channels

Effect of α_{MHD} **retained** but $\delta A_{\|}$ **ignored**.

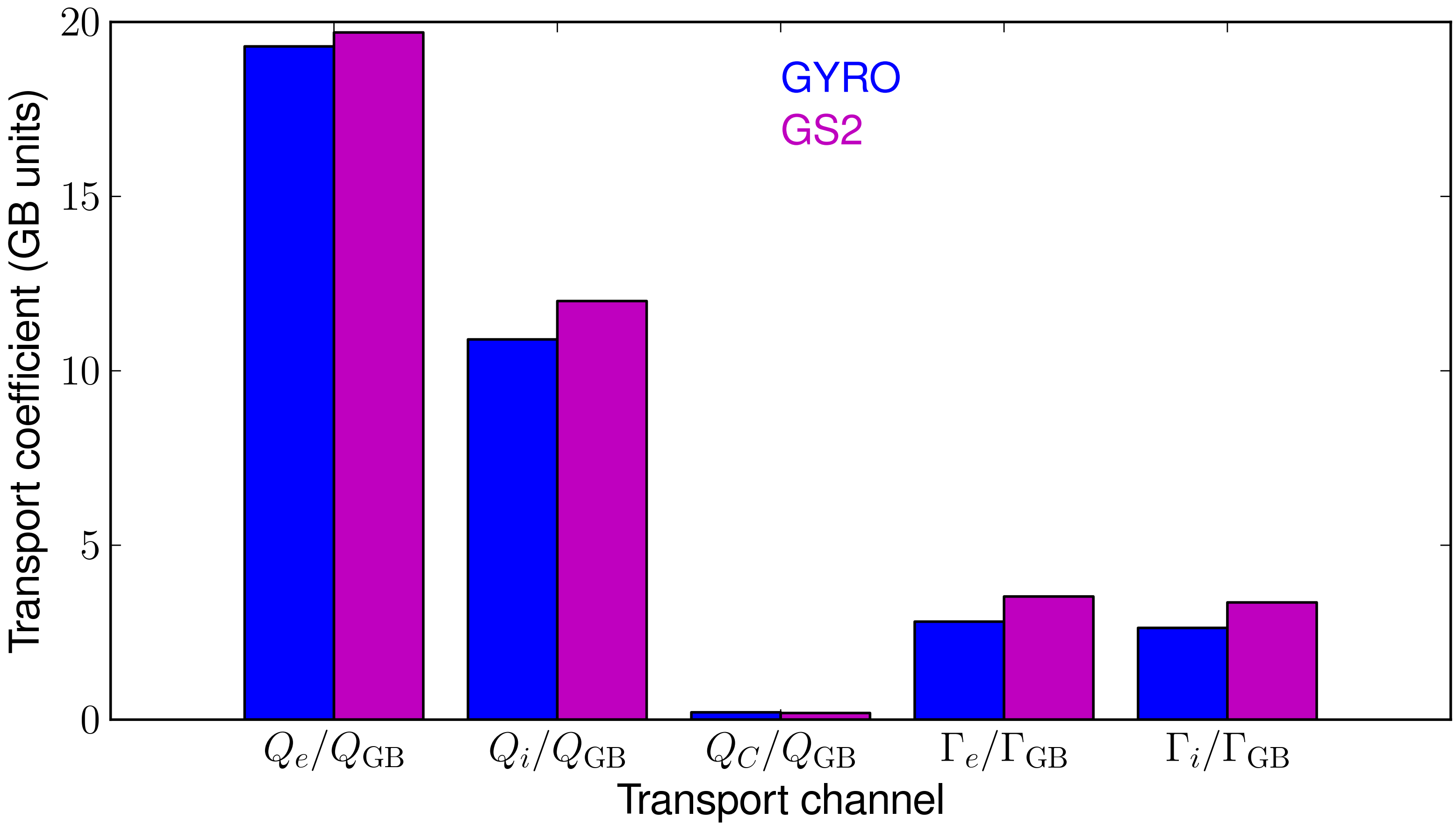

DIII-D High-β plasmas

Holland PoP 2012

- Most validation studies have focused on low-power L-mode discharges
- Key difference: $\rho_{s,\mathrm{unit}}/a$ **larger in H-mode** than L-mode
- Profile shearing effects can contribute some stabilization
- Focus on discharges created for study of transport scaling with β
- Transport in 128385 quenched at full β.

Experimental results **bracketed** by $0.5 < \beta_e/\beta_e^{\mathrm{expt}} < 1$

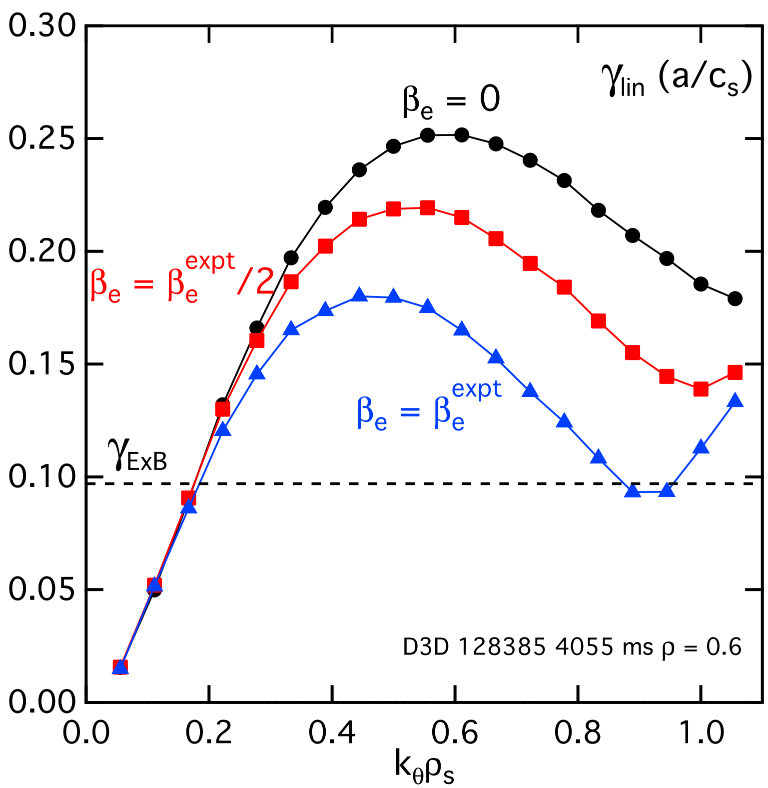

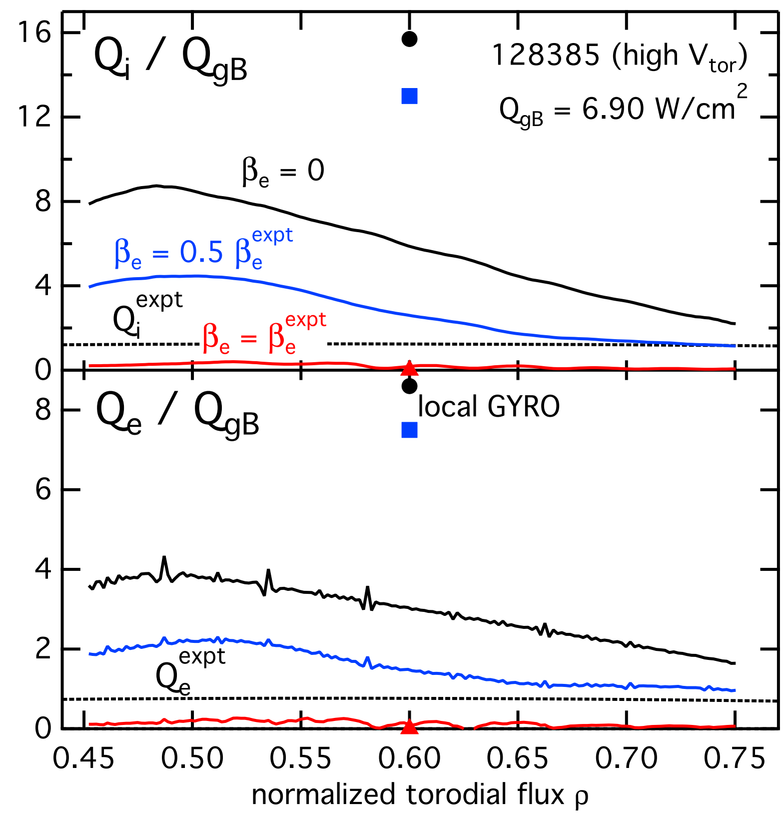

Electromagnetic Cyclone Eigenmodes including $\delta B_{\|}$

Belli POP 2010

- **Sea of modes in NSTX** made initial-value linear simulations problematic
- Near mode crossings, eigenmode fails to emerge clearly
- Impossible to generate smooth curves of frequency versus parameter.
- Creation of GYRO field **eigenvalue solver** was motivated
- This is in contrast to **Bass'** more comprehensive **distribution eigenvalue solver**

Electromagnetic Cyclone Eigenmodes including $\delta B_\parallel$

Belli POP 2010

Wavenumber scans show TEM-to-ETG transition.

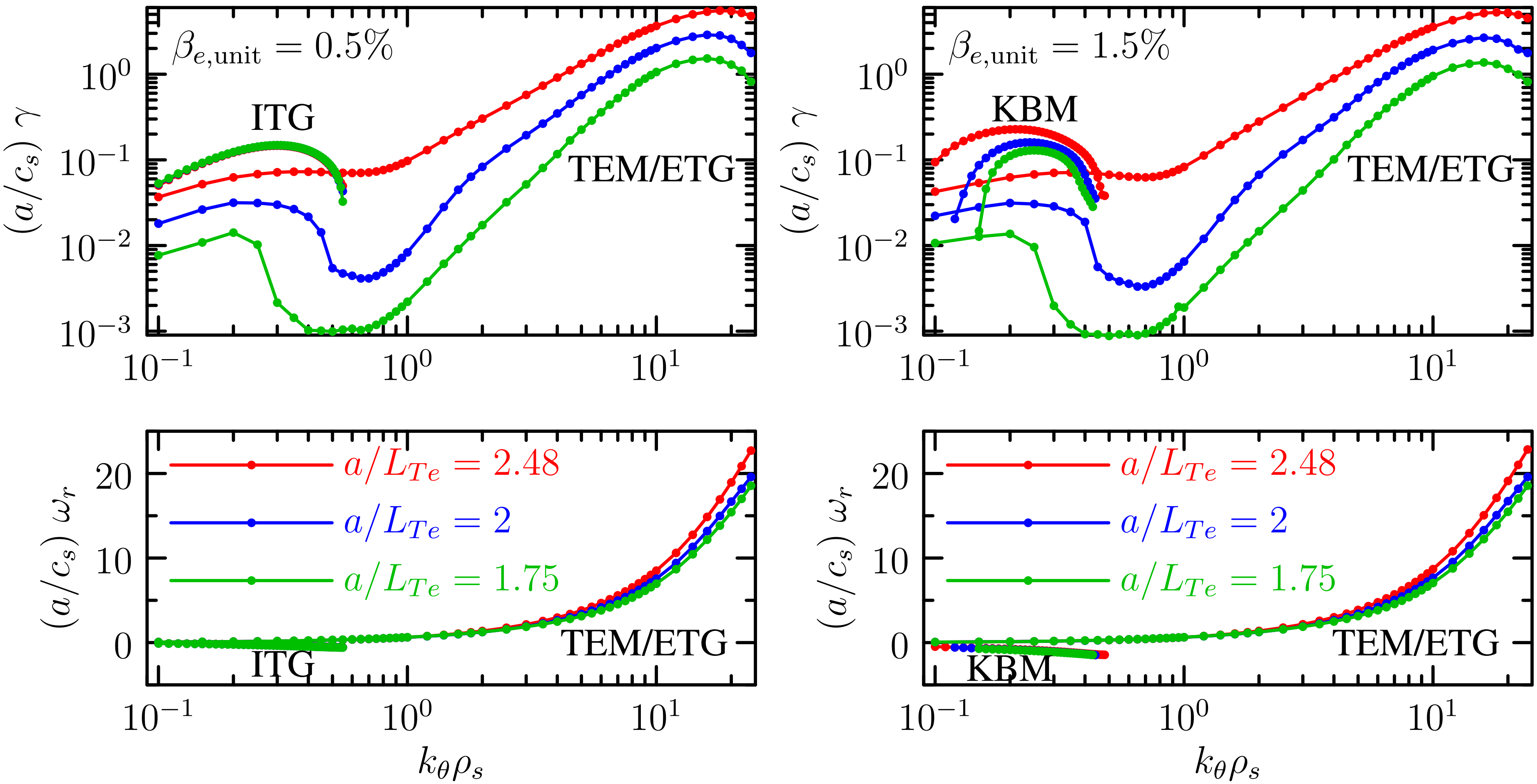

GENERAL ATOMICS

NSTX Eigenmodes at $k_\theta \rho_s = 0.25$

Belli POP 2010

(a-c): KBM, (d-i): Hybrid ITG/KBM

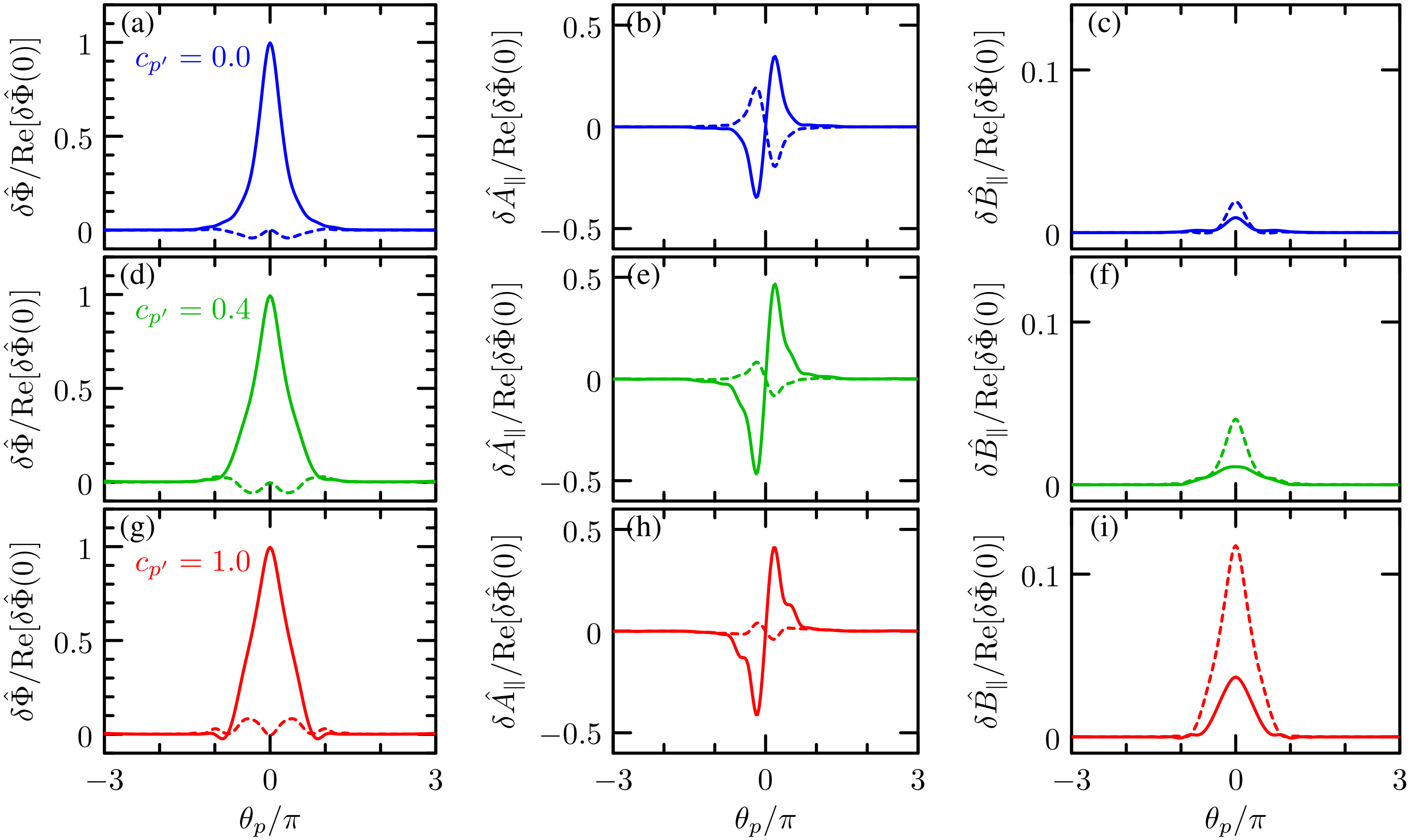

NSTX Eigenmodes at $k_\theta \rho_s = 0.6$

Belli POP 2010

(a-c): KBM, (d-f): ITG-like, (g-i): Hybrid ITG/KBM

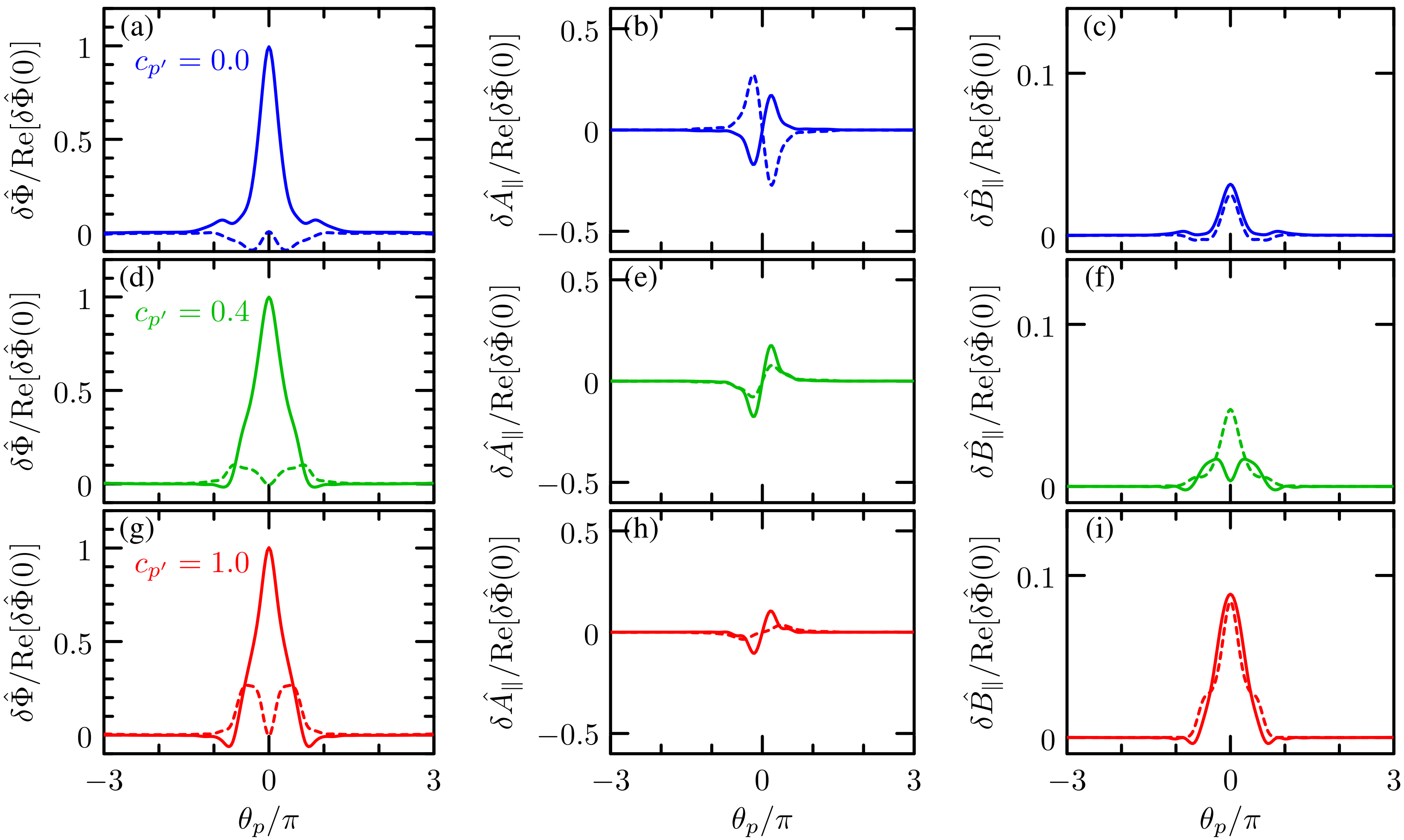

NSTX Eigenmodes at $k_\theta \rho_s = 15$

Belli POP 2010

Alfvénic drift eigenfunctions

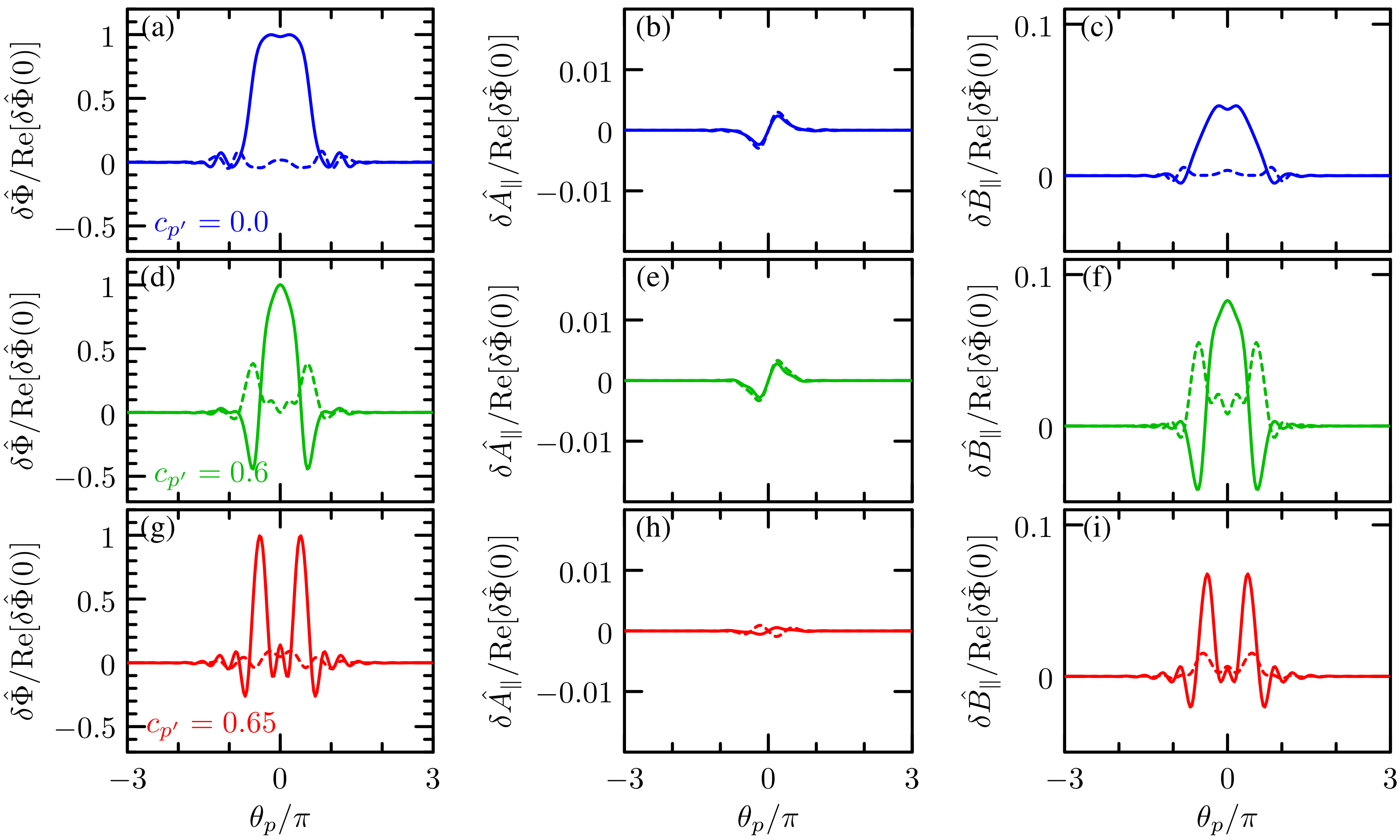

NSTX Eigenmodes at $k_\theta \rho_s = 15$

Belli POP 2010

Compressional electron drift waves

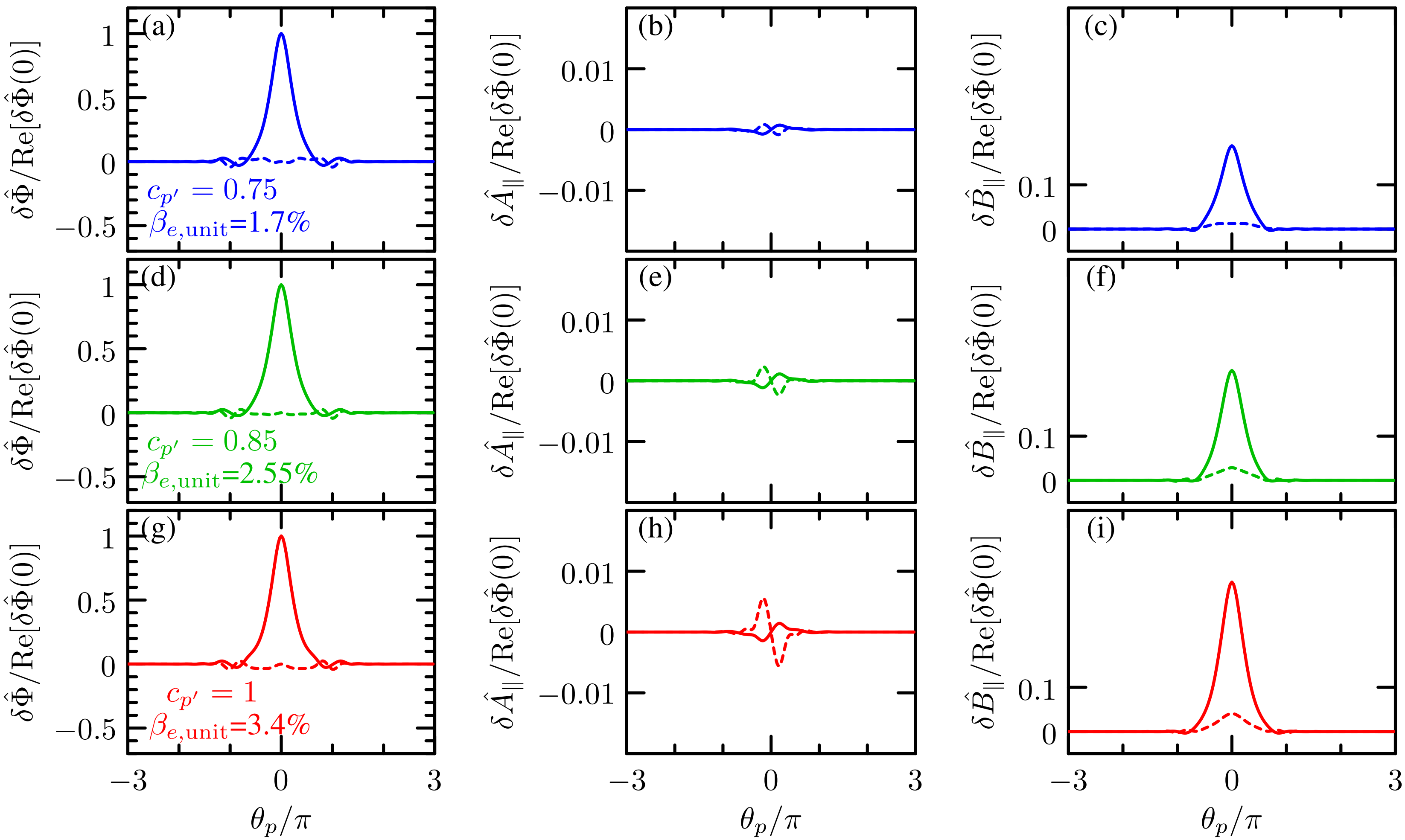

Electron energy transport in NSTX

Significant advances and innovations by Guttenfelder

- Wide range of parameters
- H-mode Q_i often near neoclassical levels
- Treat core region, $0.4 \leq r/a \leq 0.8$ with GYRO
- Electrostatic ITG/TEM found at lower β
- ETG found above $a/L_{T_e,\mathrm{crit}}$.
- Microtearing at high β_e
  - $\chi_{e,\mathrm{EM}} \simeq 6m^2/s$
  - $\Delta x \leq 0.2\rho_{s,\mathrm{unit}}$
  - Transport increases with ν_{ei}.

Electron energy transport in NSTX

129041: KBM unstable at high $\alpha_{\rm MHD} \sim \beta'$.

Ballooning mode (TEM/KBM) disappears in the absence of $\delta B_{\|}$:

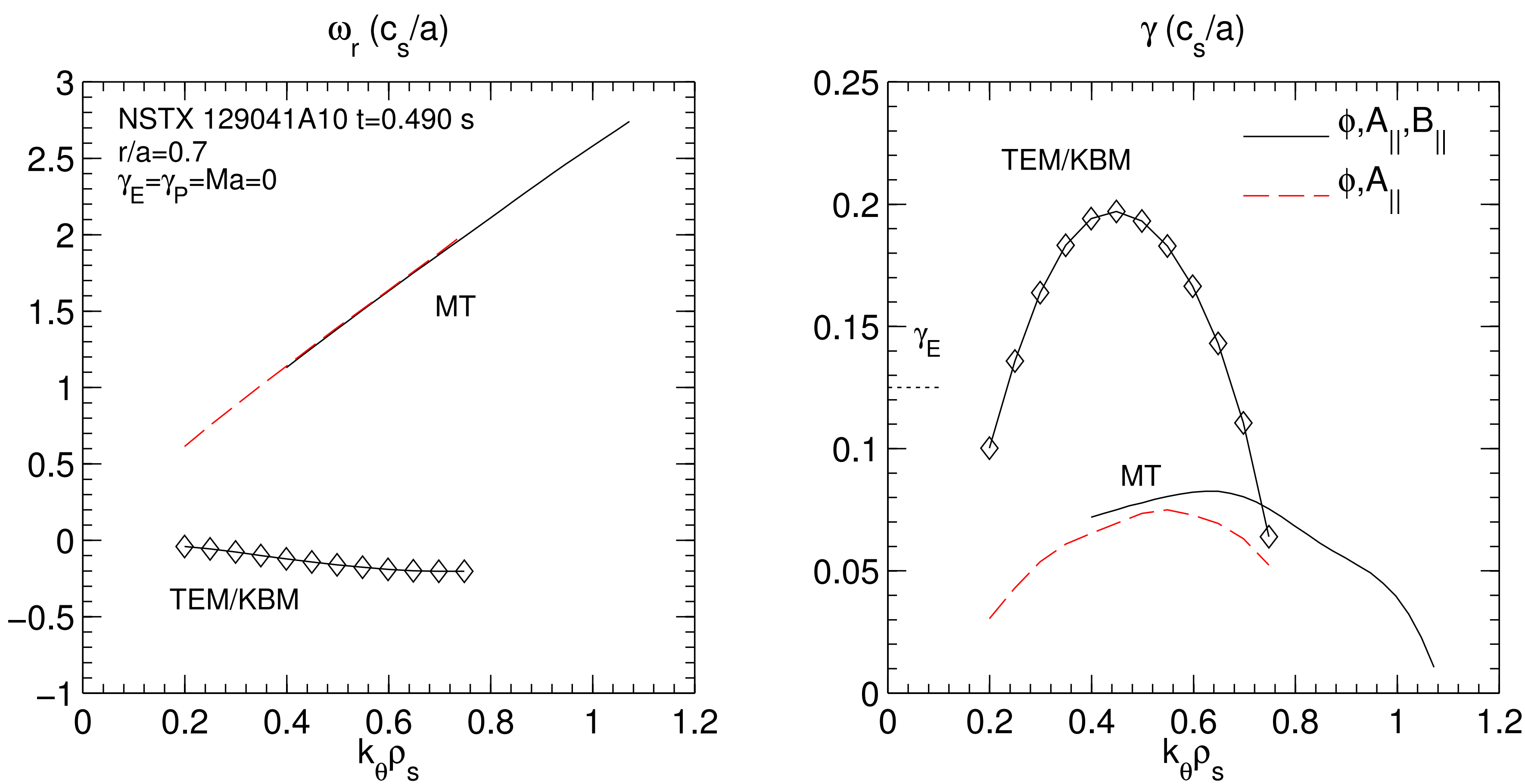

GENERAL ATOMICS

Electron energy transport in NSTX

Phenomenology of the TEM/KBM branch

TEM: Destabilized by a/L_{T_e}, a/L_n, weakly dependent on a/L_{T_i}, stabilized by ν_{ei}

KBM: Growth rate scaling unified by $\alpha_{\mathrm{MHD}} = -q^2 R\beta'$

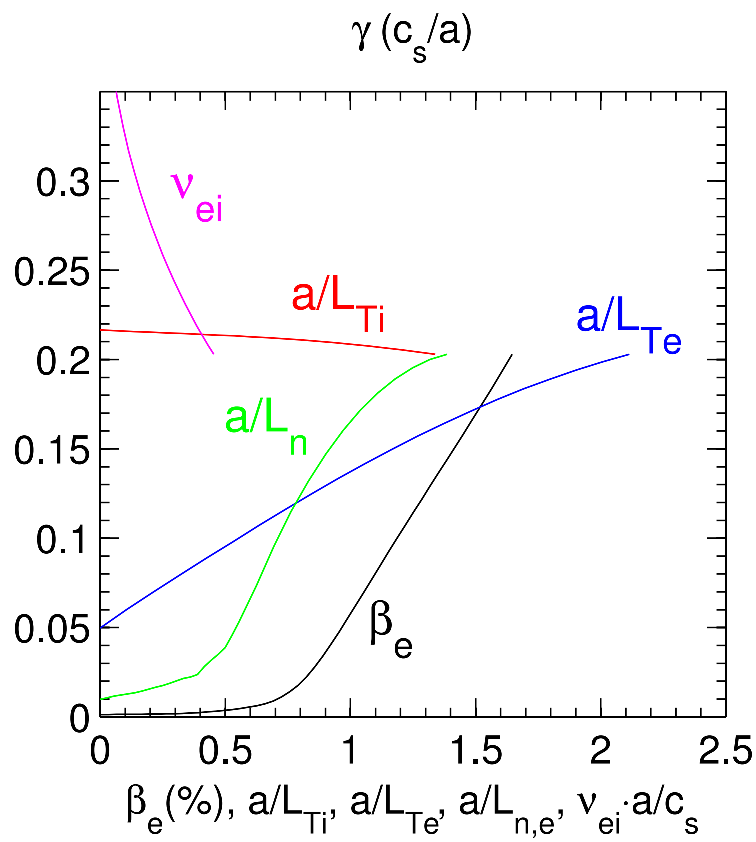

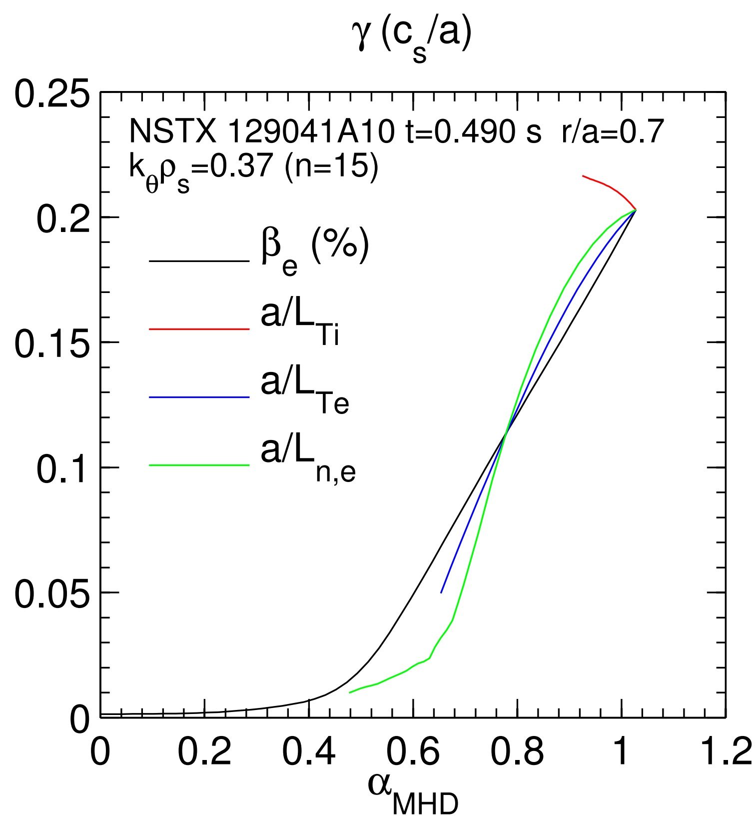

Electron energy transport in NSTX

Large contribution from compressional transport channel: $Q_e^{\delta B_\parallel}$

Nearly half of Q_e from compressional motion: $\dfrac{\delta B_\parallel}{B_\mathrm{unit}} \simeq 0.08\%$.

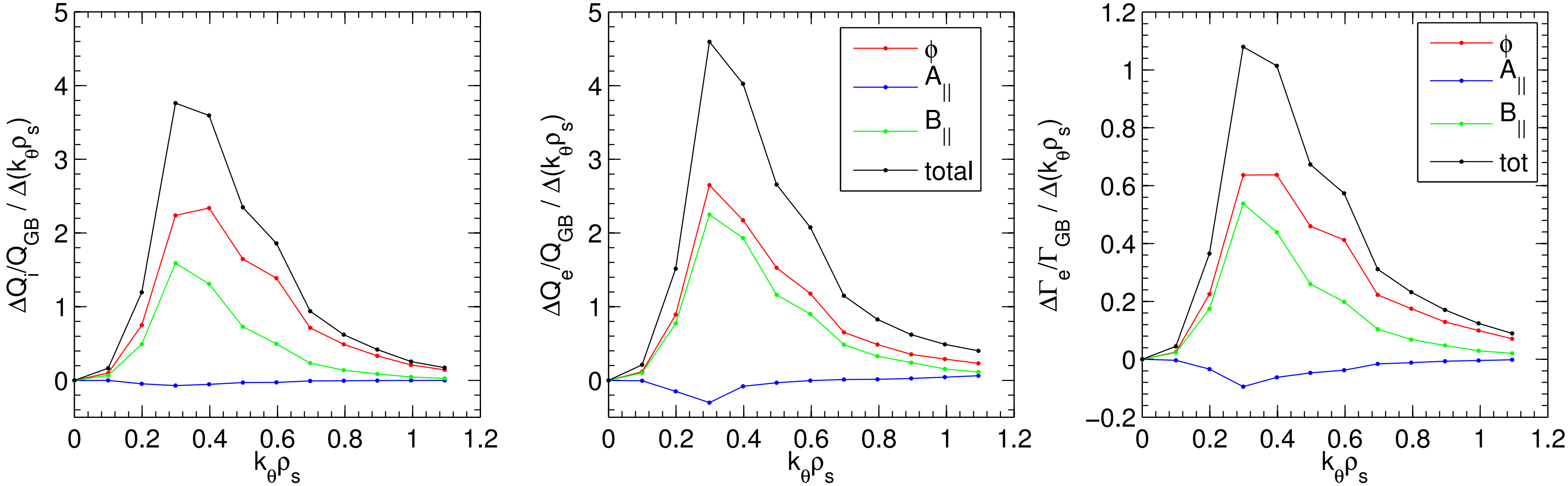

Local linear AE modes

Bass PoP 2010: Simultaneous EPM, TAE, ITG, TEM

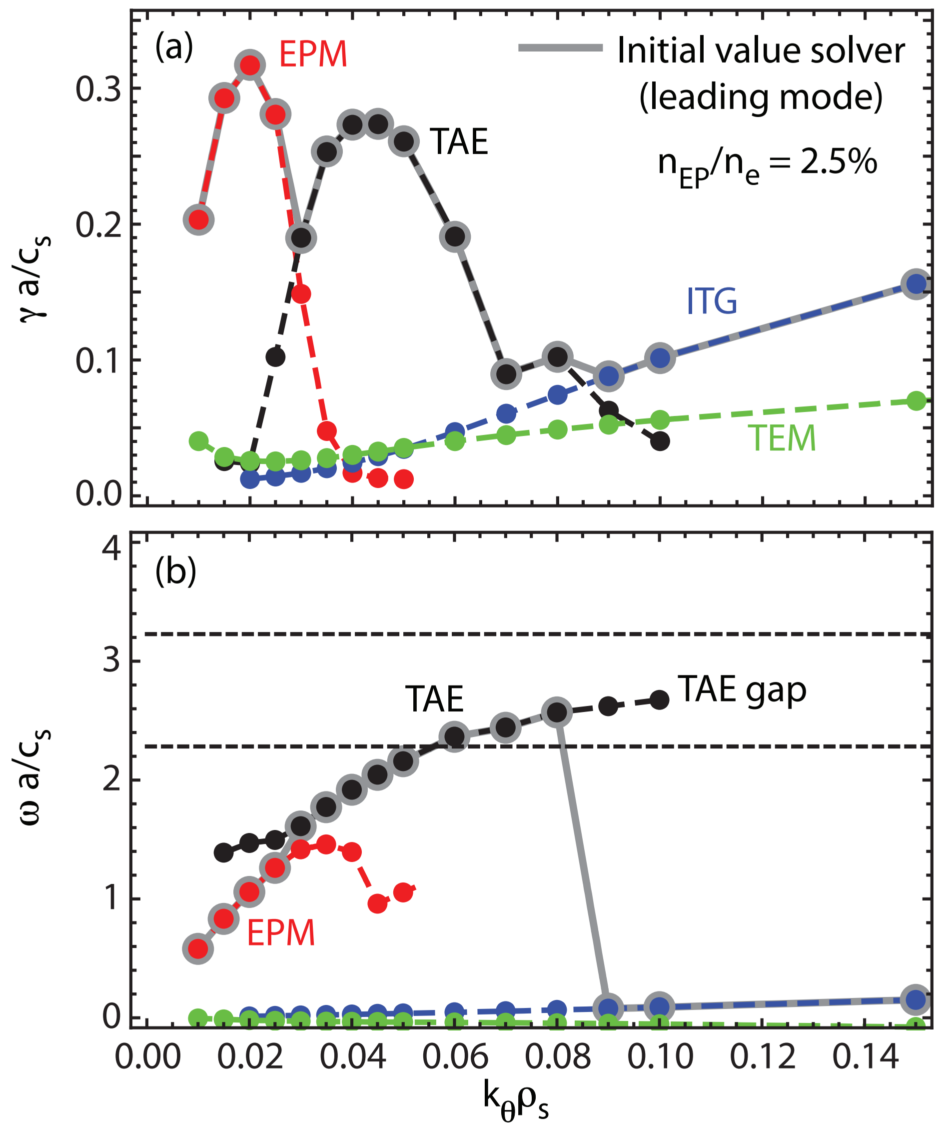

GENERAL ATOMICS

Local nonlinear AE simulations (half-torus)

Bass PoP 2010: Saturated nonlinear states at lower EP fraction

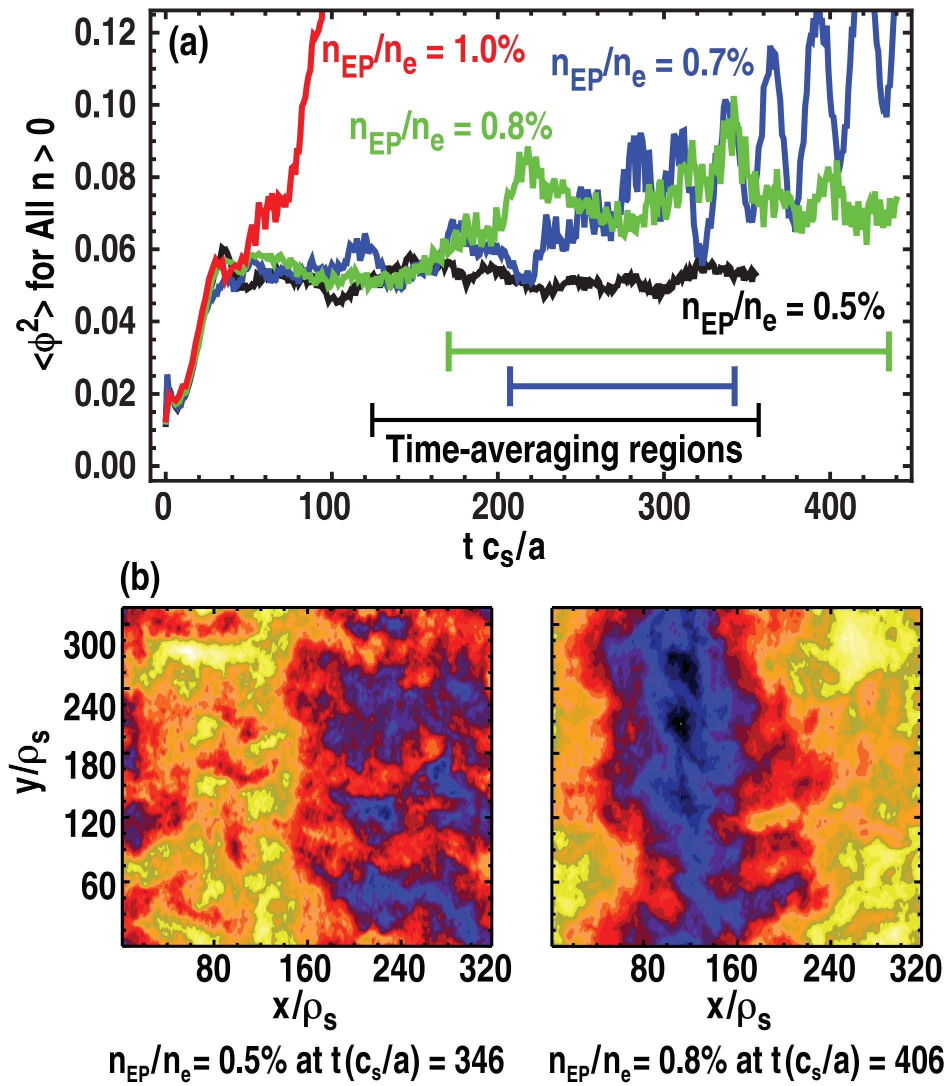

GENERAL ATOMICS

Global linear AE modes (eigenvalue solver)

Bass In Press 2012: Three simultaneous modes (DIII-D 142111)

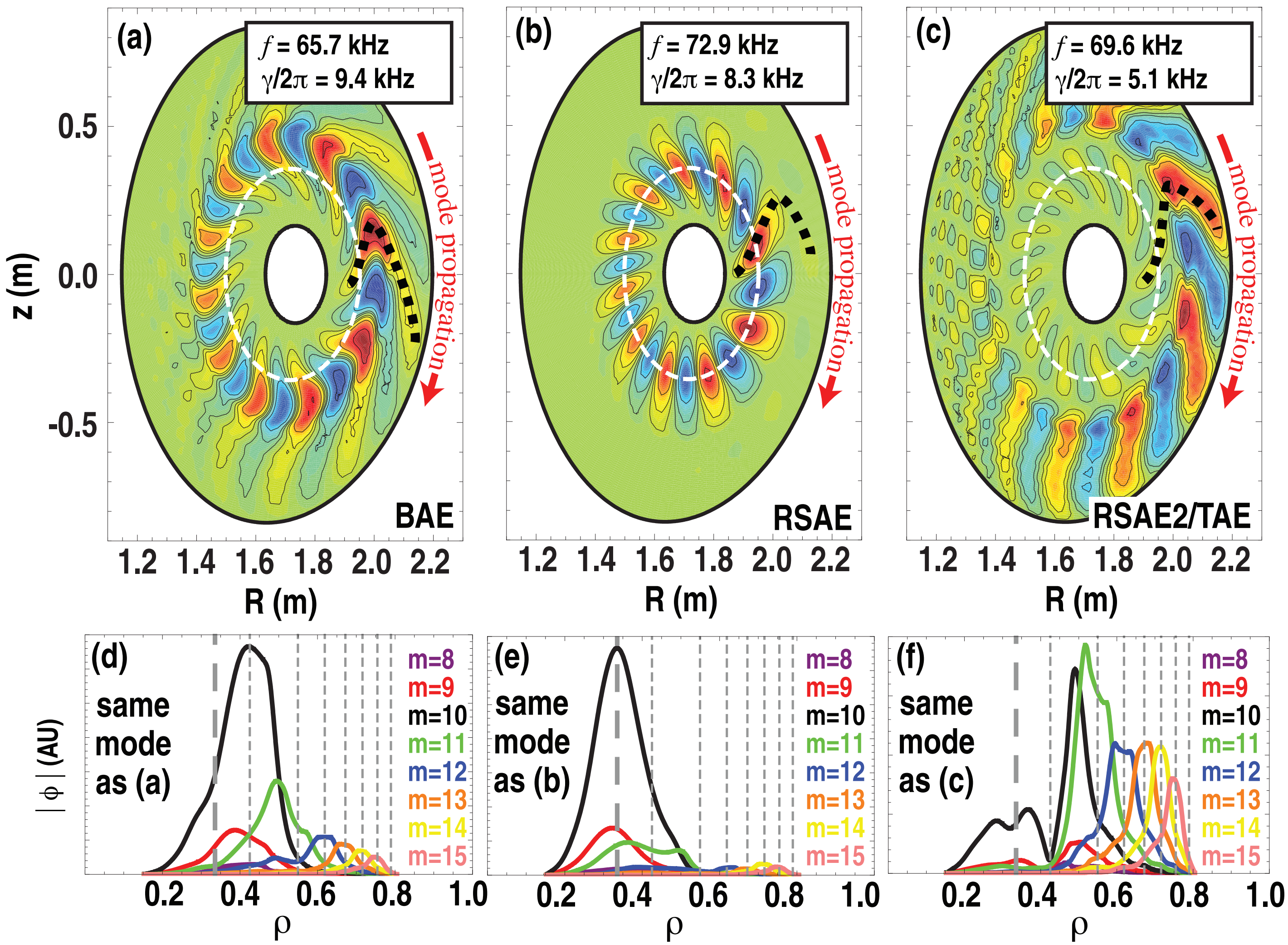

GENERAL ATOMICS

AE Simulation Challenges

Kinetic Energetic Particles

- EP orbits:
  - resolving orbit motion requires smaller timestep (factor of 10)
  - large orbits require wider gyroaverage stencil
- Near-marginality of Alfvénic modes requires long simulation times
- Multi-scale coupling requires simultaneous resolution of
  - low-k Alfvén (large domain) dynamics
  - intermediate-k ITG/TEM (fine-scale) turbulence
- Global linear analysis
  - Gyrokinetic eigensolver solves $1.15M \times 1.15M$ eigensystem!

Original β-scaling paper and the runaway

Candy POP 2005

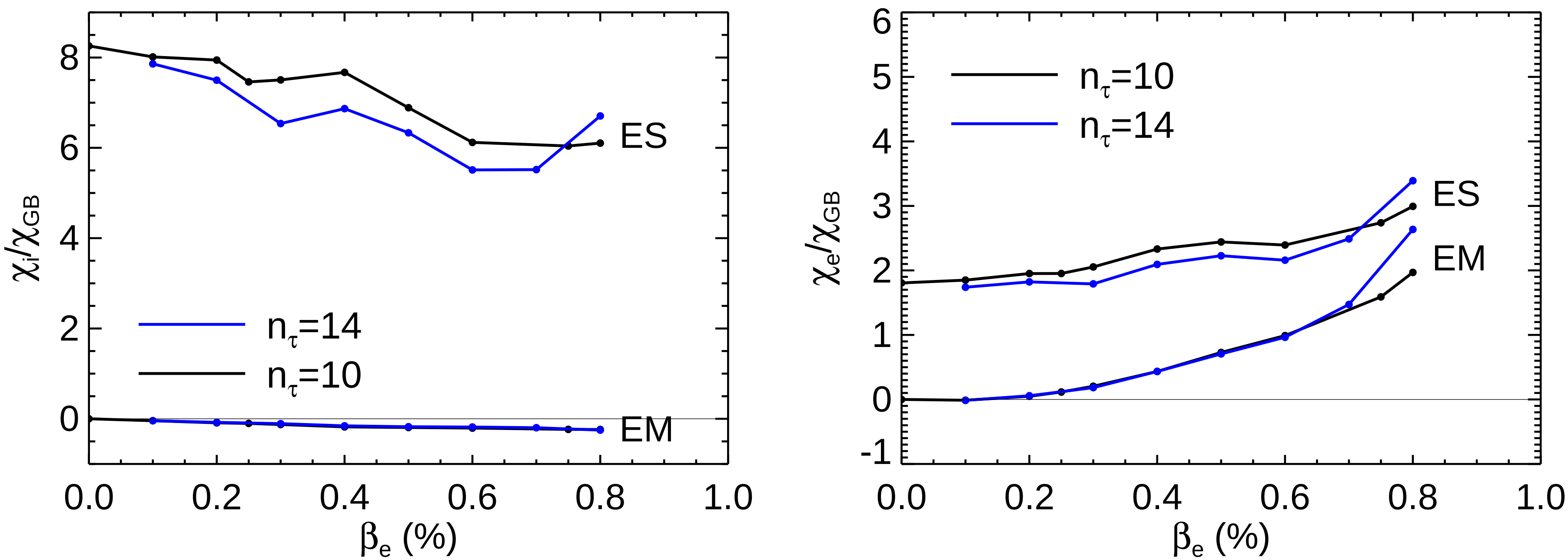

- Original β scans showed something strange happening
- Simulations **ran away** at about $\beta = (2/3)\beta_{\rm crit}$.
- Did NOT appear to be a numerical instability.

Original β-scaling paper and the runaway

Candy POP 2005

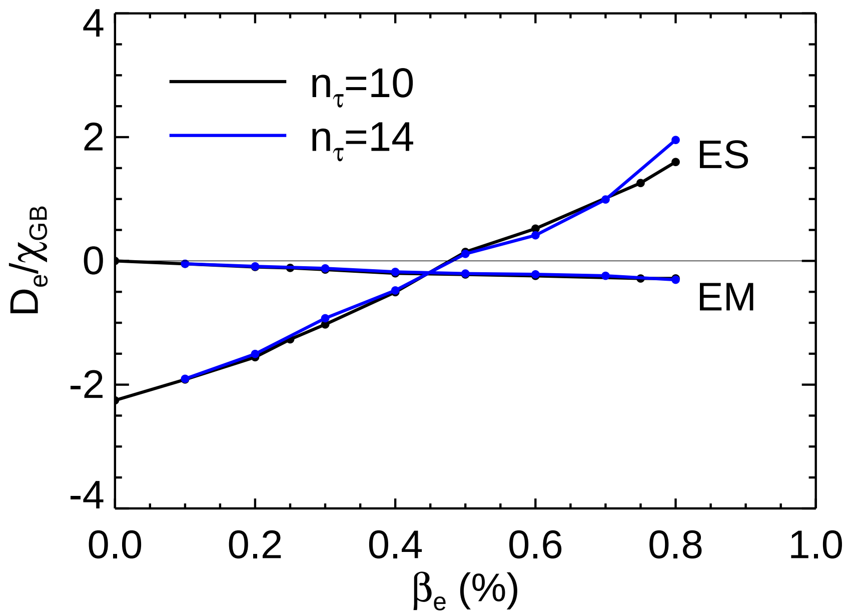

- Runaway motivated the development of the IMEX-RK semi-implicit method.
  - Wasn't a miracle cure
  - SIDE-BENEFIT: linear simulations with real m_i/m_e much faster
- Cancellation issue eventually ruled out as culprit

GENERAL ATOMICS

Original β-scaling paper and corrugations

Candy POP 2005

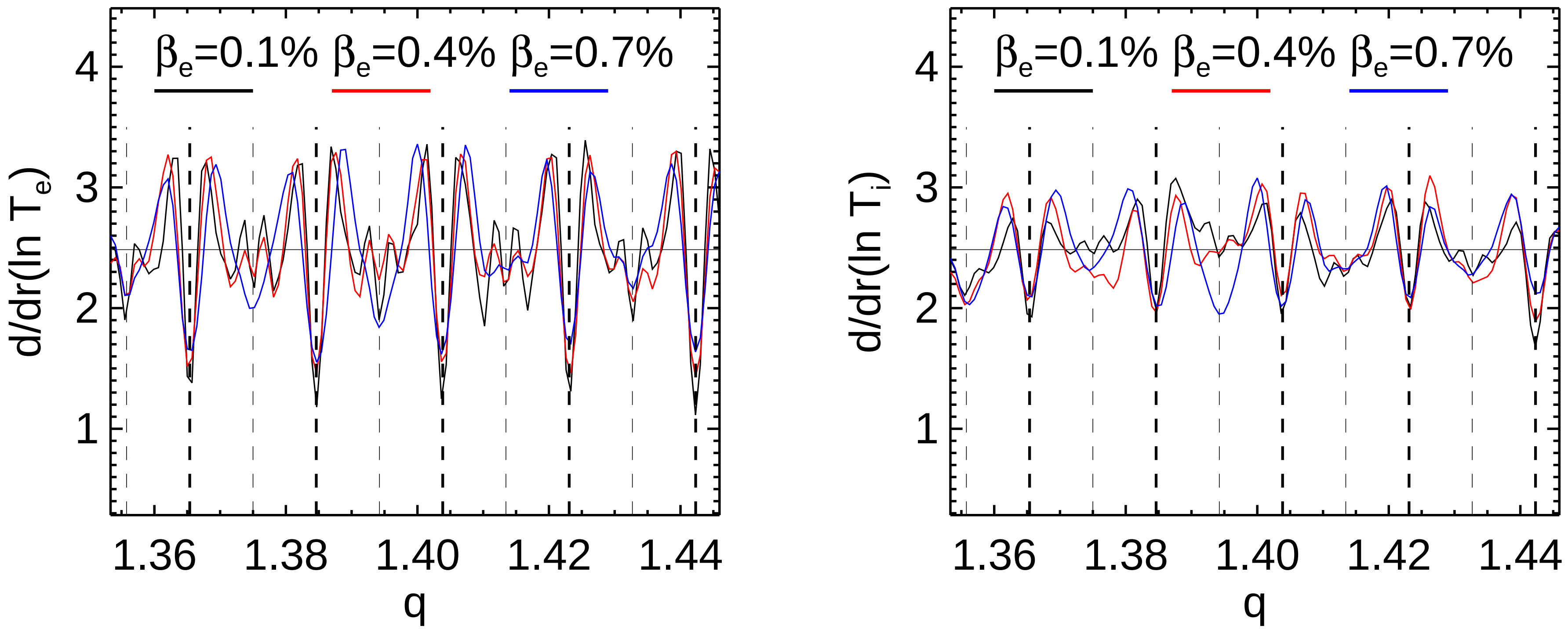

- Significant radial structure about lowest-order rational surfaces
- Related to full (non-fluid) kinetic electron response
- Physical pole-like structure in electron propagator

Electromagnetic Fluctuations and Magnetic Stochasticity

- Connection between **runaway** and **stochasticity** was suggested *ca.* 2006
- Quantification required magnetic-field-line **mapping capability**
- Tedious because of ballooning representation
- Poincaré mapper part of GYRO: `gacode/gyro/tools/fieldline`
- There were various **diversions** related to runaway "cures"
  - better numerical methods
  - more physical realism (collisions)
  - higher resolution (electron-scale grid)
- Runaway is **correct solution** of model equations

Electromagnetic Fluctuations and Magnetic Stochasticity

Wang POP 2011, PRL 2011

- **GYRO, GENE and GKW** were ultimately in **agreement** about the runaway

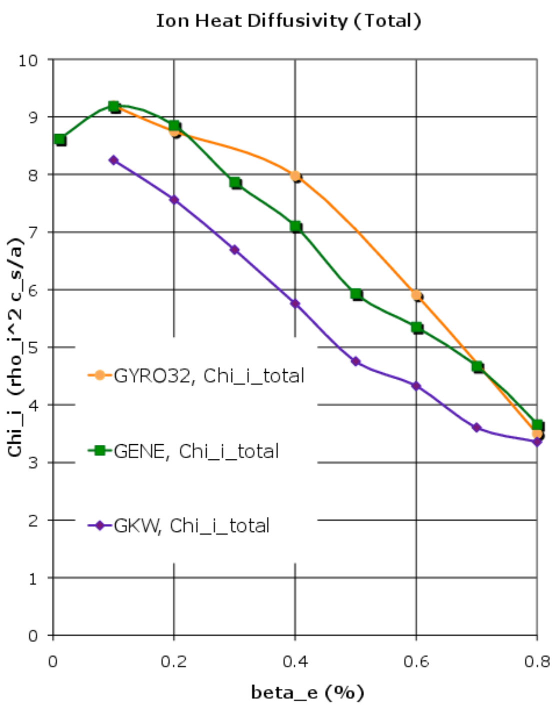

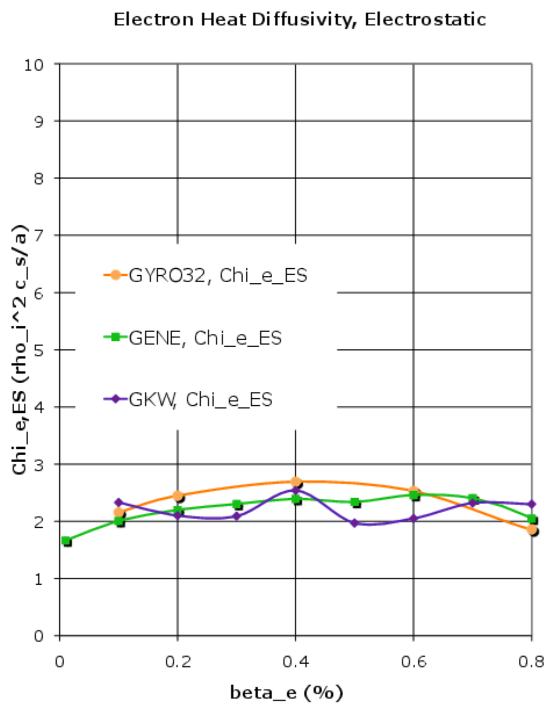

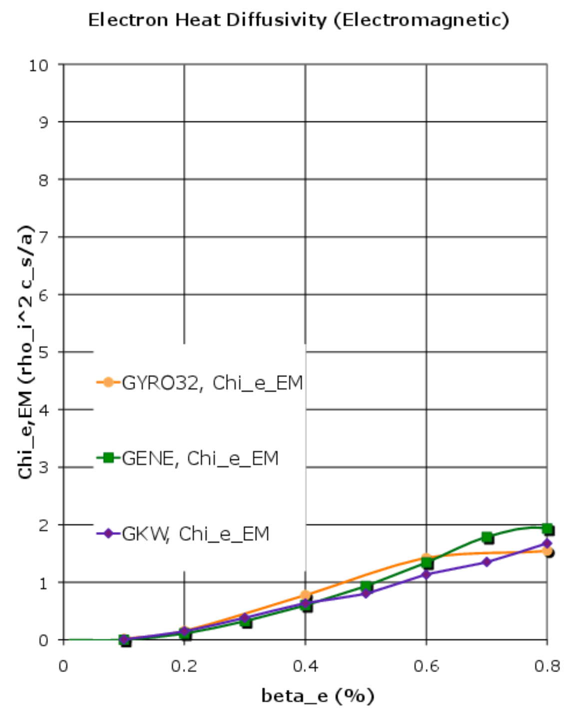

GENERAL ATOMICS

Magnetic Stochasticity

Wang POP 2011, PRL 2011

- **Remarkable discovery 1:** Stochasticity observed at smallest values of β
- Chaos in this case is not "simple"; appear to be bounding tori.

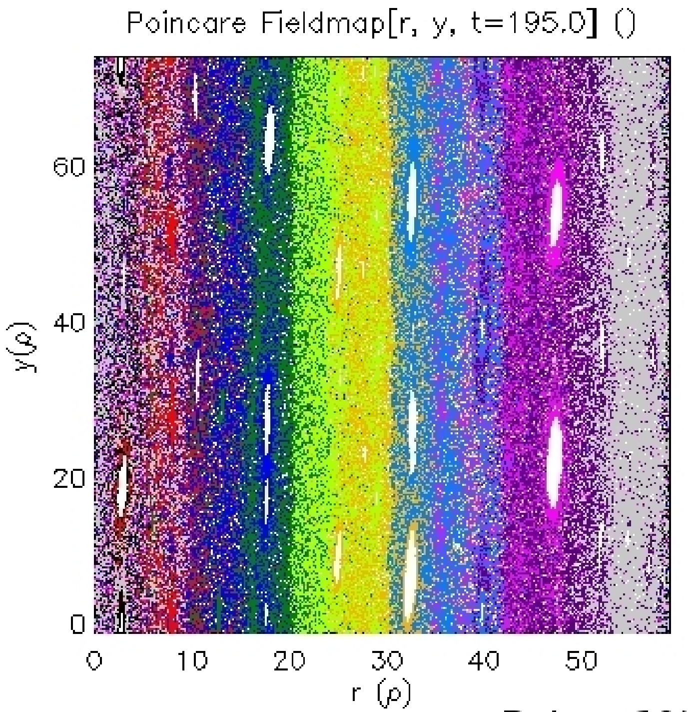

Beta=.1%

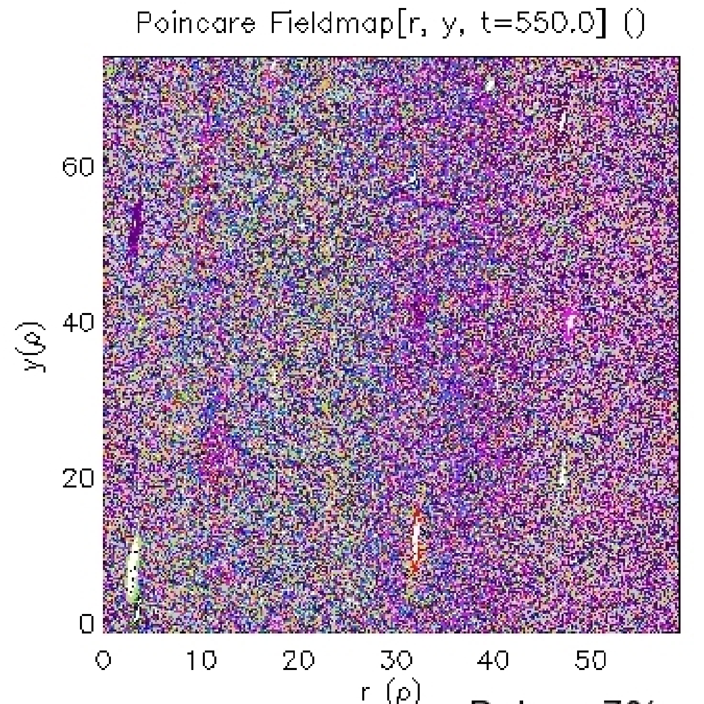

Beta=.7%

Magnetic Stochasticity

Wang POP 2011, PRL 2011

- **Remarkable discovery 2:** EM electron transport is almost purely chaotic
- Correlation in time suprisingly high

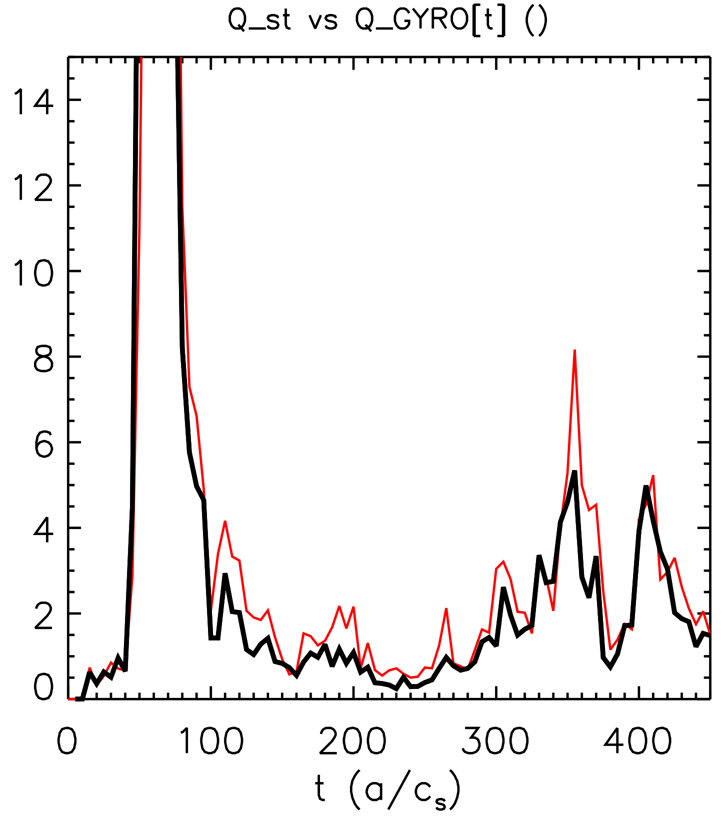

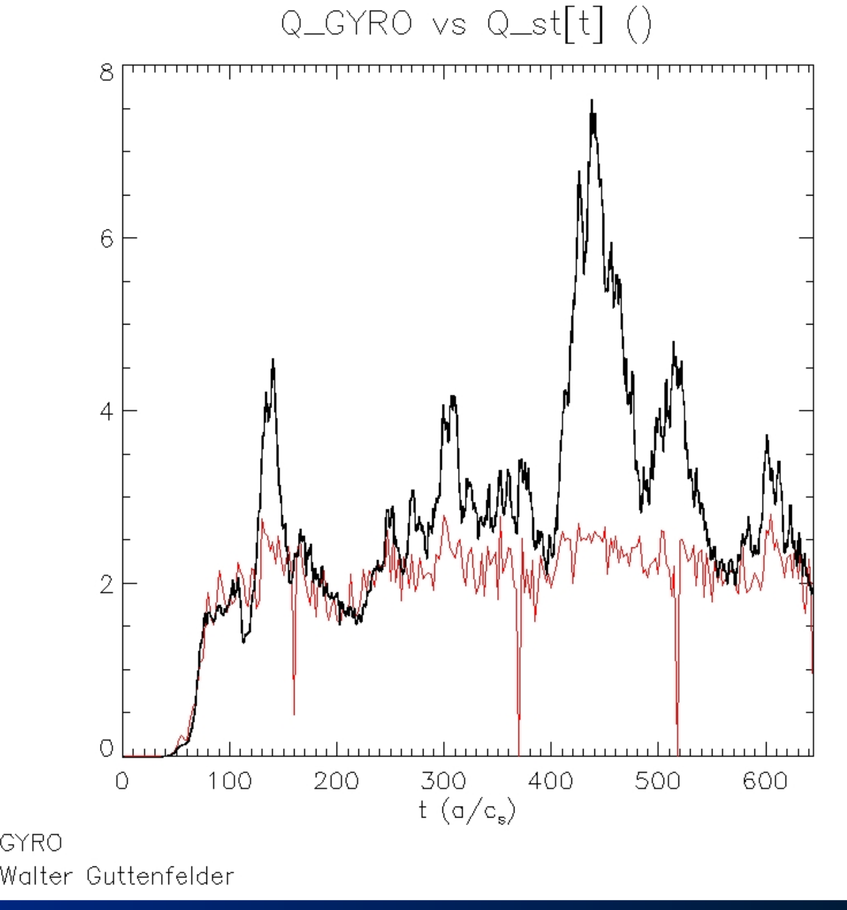

GENERAL ATOMICS

Magnetic Stochasticity

Wang POP 2011, PRL 2011

- Stochastic energy flux, $Q_{\rm st}$, is stochastic particle flux, d_m, times tentative conversion factor:

$$Q_{\rm st} = \sqrt{\frac{8}{\pi}} d_m \frac{v_{\rm th}}{L_T} n_{\rm pass} T$$

- Bursts in NSTX (Guttenfelder) not understood

Subcritical MHD β-limit

Waltz POP 2010

- Total pressure profile **corrugated** at finite transport levels
- Some evidence that regions of larger p' lower the **effective β limit**

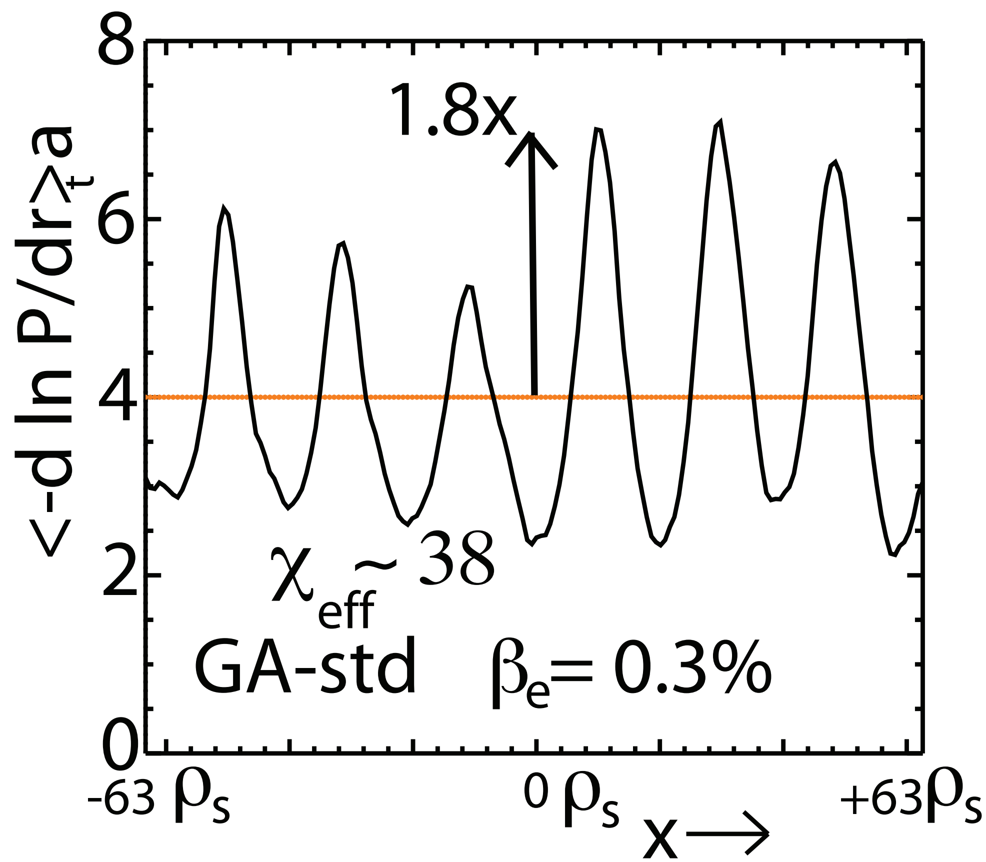

GENERAL ATOMICS